AD-A200 066

DTIC FILE COPY

(1)

DURABILITY AND DAMAGE TOLERANCE OF ALUMINUM CASTINGS

M.W. OZELTON
G.R. TURK

DTIC
ELECTE
OCT 0 5 1988
S D
D

NORTHROP CORPORATION
AIRCRAFT DIVISION
ONE NORTHROP AVENUE
HAWTHORNE, CALIFORNIA 90250

September 1988
NOR 88-23

Second Interim Technical Report
For Period June 1987 - May 1988
Contract No. F33615-85-C-5015

Approved For Public Release: Distribution Unlimited

Prepared For:
MATERIALS LABORATORY
AIR FORCE WRIGHT AERONAUTICAL LABORATORIES
WRIGHT-PATTERSON AFB, OHIO 45433-6533

88 10 4 108

UNCLASSIFIED
SECURITY CLASSIFICATION OF THIS PAGE

REPORT DOCUMENTATION PAGE

1a. REPORT SECURITY CLASSIFICATION Unclassified	1b. RESTRICTIVE MARKINGS
2a. SECURITY CLASSIFICATION AUTHORITY	3. DISTRIBUTION / AVAILABILITY OF REPORT Unlimited
2b. DECLASSIFICATION / DOWNGRADING SCHEDULE	
4. PERFORMING ORGANIZATION REPORT NUMBER(S) NOR 88-23	5. MONITORING ORGANIZATION REPORT NUMBER(S)
6a. NAME OF PERFORMING ORGANIZATION Northrop Corporation Aircraft Division 6b. OFFICE SYMBOL (If applicable) 3872/62	7a. NAME OF MONITORING ORGANIZATION Air Force Wright Aeronautical Laboratories
6c. ADDRESS (City, State, and ZIP Code) One Northrop Avenue Hawthorne, CA 90250	7b. ADDRESS (City, State, and ZIP Code) AFWAL/MLSE Wright-Patterson AFB, OH 45433
8a. NAME OF FUNDING / SPONSORING ORGANIZATION Air Force Wright Aeronautical Laboratories 8b. OFFICE SYMBOL (If applicable)	9. PROCUREMENT INSTRUMENT IDENTIFICATION NUMBER F33615-85-C-5015
8c. ADDRESS (City, State, and ZIP Code) Wright-Patterson AFB, OH 45433	10. SOURCE OF FUNDING NUMBERS PROGRAM ELEMENT NO / PROJECT NO / TASK NO / WORK UNIT ACCESSION NO

11. TITLE (Include Security Classification)
Durability and Damage Tolerance of Aluminum Castings (Unclassified)

12. PERSONAL AUTHOR(S) M. W. Ozelton and G. R. Turk

13a. TYPE OF REPORT	13b. TIME COVERED	14. DATE OF REPORT (Year, Month, Day)	15. PAGE COUNT
Interim	FROM 6/1/87 TO 5/31/88	1988, September	76

16. SUPPLEMENTARY NOTATION

17. COSATI CODES		
FIELD	GROUP	SUB-GROUP

18. SUBJECT TERMS (Continue on reverse if necessary and identify by block number)
Aluminum castings, ~~D357, B201~~, mechanical properties, durability, damage tolerance, equivalent initial flaw size, fatigue, fracture toughness.

19. ABSTRACT (Continue on reverse if necessary and identify by block number)

A durability and damage tolerance property data base for D357-T6 and B201-T7 cast by three commercial foundries was developed. The specifications for the two alloys were selected based on the results of screening evaluations which are included in the first interim report published in September 1987.

Tensile, fatigue, and fracture toughness properties were determined and microstructural and fractographic evaluations were conducted. The fatigue data (stress-life and crack growth rate) were used to calculate an equivalent initial flaw size for both alloys and will be used to assess the applicability of current DADT specifications to castings.

20. DISTRIBUTION / AVAILABILITY OF ABSTRACT ☐ UNCLASSIFIED/UNLIMITED ☒ SAME AS RPT ☐ DTIC USERS	21. ABSTRACT SECURITY CLASSIFICATION Unclassified
22a. NAME OF RESPONSIBLE INDIVIDUAL	22b. TELEPHONE (Include Area Code) / 22c. OFFICE SYMBOL

DD FORM 1473, 84 MAR — 83 APR edition may be used until exhausted. All other editions are obsolete.

SECURITY CLASSIFICATION OF THIS PAGE
Unclassified

ABSTRACT

A durability and damage tolerance property data base was developed for D357-T6 and B201-T7 alloys that were cast by three commercial foundries. The specifications for the two alloys were selected based on the results of screening evaluations which are included in the first interim report published in September, 1987.

Tensile, fatigue, and fracture toughness properties were determined and microstructural and fractographic evaluations were conducted. Fatigue data (stress-life and crack growth rate) for both alloys were used to calculate an equivalent initial flaw size, which will be used to assess the applicability of current DADT specifications to castings.

COPY INSPECTED 4

Accesion For
NTIS CRA&I ✓
DTIC TAB
Unannounced
Justification
By
Distribution/
Availability Codes
Dist | Avail and/or Special
A-1

PREFACE

This second interim report covers the work performed under Contract F33615-85-C-5015 from June 1987 to May 1988 by Northrop Corporation, Aircraft Division, Hawthorne, California, under Project Number 2418. The program is administered under the technical direction of Mary Ann Phillips, AFWAL/MLSE, Wright-Patterson AFB, Ohio 45433.

The work is being performed by Northrop's Metallic Materials and Processes Research and Development Department. Dr. M. W. Ozelton is the Program Manager and Mr. G. R. Turk is the Principal Investigator. The contributions of the following people are acknowledged: P. G. Porter, equivalent initial flaw size analyses; K. J. Oswalt for many invaluable discussions; S. Hsu, mechanical testing; D. R. Drott, H. E. Langman, and M. A. Arrieta for coordinating and carrying out the many and varied activities to obtain the test data; and J. F. Williams for preparing the manuscript.

The major subcontractors for the program are Alcoa, Premium Castings Division, Corona, California; Hitchcock Industries Inc., Minneapolis, Minnesota; Fansteel Wellman Dynamics, Creston, Iowa; and Dr. L. Adler of Ohio State University (NDI consultant).

CONTENTS

SECTION		PAGE
1	INTRODUCTION	1
2	OBJECTIVE	3
3	PROGRAM APPROACH	5
4	EXPERIMENTAL PROCEDURES	9
	4.1 PRODUCTION OF CASTINGS	9
	4.2 TEST PROCEDURES	20
	4.3 EQUIVALENT INITIAL FLAW SIZE ANALYSIS	22
5	RESULTS AND DISCUSSION	27
	5.1 D357-T6	27
	5.1.1 Composition	28
	5.1.2 Microstructure	28
	5.1.3 Tensile Properties	35
	5.1.4 Fatigue Properties	37
	5.1.5 Fracture Toughness	39
	5.1.6 Equivalent Initial Flaw Size	43
	5.2 B201-T7	50
	5.2.1 Composition	50
	5.2.2 Microstructure	50
	5.2.3 Tensile Properties	55
	5.2.4 Fatigue Properties	57
	5.2.5 Fracture Toughness	60
	5.2.6 Stress Corrosion	60
	5.2.7 Equivalent Initial Flaw Size	63
6	CONCLUSIONS	67
7	REFERENCES	69

LIST OF FIGURES

FIGURE PAGE

1 Program Outline.....6

2 Rigging System Used by Foundry A to Produce D357 Plates.....13

3 Rigging System Used by Foundry B to Produce D357 Plates.....15

4 Rigging System Used by Foundry C to Produce B201 Plates.....19

5 Typical D357-T6 Microstructure.....30

6 Backscatter SEM Micrograph of D357-T6.....33

7 TEM Micrograph of D357-T6 Showing Si Particles.....33

8 TEM Micrograph of D357-T6 Showing a Needle-Shaped Phase Containing Ti.....33

9 (a) TEM Micrograph of D357-T6 Showing a Needle-Shaped Particle Containing Ti and Smaller Mg_2Si Particles.....34

(b) Selected Area Diffraction Pattern of the Needle Phase of Figure 9(a).....34

10 D357-T6 Stress-Life Fatigue Data.....38

11 D357-T6 Strain-Life Fatigue Data.....38

12 D357-T6 Fatigue Crack Growth Rate Data.....40

13 Typical Crack Initiation Sites in D357-T6 Fatigue Specimens.....41

14 Relationship Between Fracture Toughness and Yield Strength for D357-T6.....44

15 Weibull Distribution of D357-T6 EIFS Data.....47

16 Measured Area of Defect Size in D357-T6.....49

17 Typical B201-T7 Microstructure.....51

18 TEM Micrograph of B201-T7 Showing the Theta Phase.....53

19 Backscatter SEM Image of B201-T7.....54

LIST OF FIGURES

FIGURE PAGE

20 STEM Micrograph of B201-T7 Showing a Phase Rich in Al, Cu, Fe, and Mn....54

21 TEM Micrograph of B201-T7 Showing a Phase Rich in Al, Cu, and Mn....54

22 TEM Micrograph of B201-T7 Showing a Phase Rich in Al and Ti....54

23 B201-T7 Stress-Life Fatigue Data....58

24 B201-T7 Strain-Life Fatigue Data....58

25 B201-T7 Fatigue Crack Growth Rate Data....59

26 Foreign Material on a B201-T7 Fatigue Specimen Fracture Surface....61

27 Relationship Between Fracture Toughness and Yield Strength of B201-T7....62

28 Weibull Distribution of B201-T7 EIFS Data....65

LIST OF TABLES

TABLE		PAGE
1	Composition Specification for the D357-T6 Verification Plates	11
2	Composition Specification for the B201-T7 Verification Plates	16
3	Verification Tests for D357-T6 and B201-T7	21
4	D357 Verification Material Melt Compositions	29
5	D357 DAS and Si Particle Data	31
6	Tensile Properties of 1.25-inch-thick, Water- and Glycol-quenched D357-T6 Plates	36
7	Fatigue Crack Initiation Sites for D357-T6 Fatigue Specimens	40
8	D357-T6 Fracture Toughness Data	42
9	D357-T6 Equivalent Initial Flaw Size Data	45
10	Comparison of Predicted and Measured Equivalent Initial Flaw Size for D357-T6	48
11	B201 Verification Material Melt Compositions	51
12	Tensile Properties of 1.25-inch-thick B201-T7 Plates	56
13	B201-T7 Fracture Toughness Data	62
14	B201-T7 Equivalent Initial Flaw Size Data	64
15	Comparison of Predicted and Measured Equivalent Initial Flaw Size for B201-T7	66

SECTION 1
INTRODUCTION

The use of castings for aircraft applications offers the potential for significant cost and weight savings compared with built-up structures. Recurring cost reductions greater than 30 percent are possible through reduced machining and assembly costs. Weight savings can be achieved, for example, by eliminating lap joints and fasteners. A reduction in fastener holes decreases the number of potential flaw initiation sites. Castings also allow greater shape flexibility compared with built-up structures.

Castings are not currently used in fatigue-critical aircraft structure because of the inability to accurately inspect thick sections, and a lack of durability and damage tolerance (DADT) data and design allowables that take into account the effects of inherent casting discontinuities and microstructural features on DADT properties. The absence of the required DADT data for castings precludes compliance with the current military DADT specifications, MIL-A-83444 and MIL-A-87221. As a result, it is not possible to take advantage of the inherent cost and weight savings of castings for fatigue-critical aircraft applications.

The goals of the "Durability and Damage Tolerance of Aluminum Castings" (DADTAC) program are to (a) investigate a nondestructive inspection (NDI) technique that has the potential for providing a quantitative assessment of the discontinuities present in aluminum castings, (b) identify the process variables and discontinuities that influence the DADT properties, and (c) characterize the DADT properties of the aluminum casting alloys A357 and A201. On completion of the program, revisions to material, process, and DADT specifications will be recommended, if necessary.

The first interim report [1] covered work conducted during the first 21 months of the program under Tasks 1 and 2 of Phase I. NDI investigations and the effects of process variables on the properties of A357-T6 and A201-T7 castings were described. This second interim report covers additional work conducted during the following 12 months under Task 2 of Phase I (see Section 3 for further details). Tensile, microstructural, and durability and damage tolerance properties of A357-T6 and A201-T7 produced using the specifications selected earlier [1] in Task 2 were determined. These alloys were produced according to AMS specifications 4241 [2] and 4242 [3], respectively, though a requirement for a silicon modifier was added to AMS 4241. Therefore, A357 and A201 will be referred to as D357 and B201, respectively, throughout this report, per the AMS specifications.

SECTION 2
OBJECTIVE

The overall objective of the DADTAC program is to generate durability and damage tolerance data for premium quality aluminum castings and advance foundry technology to expedite the use of these castings in primary aircraft structures. In addition, recommendations for modifying material, process, and DADT specifications will be made as required.

SECTION 3
PROGRAM APPROACH

The DADTAC program, which consists of three phases, is summarized in Figure 1. A brief description of the technical activities associated with each phase is provided below.

Phase I - DADT of Aluminum Castings Quality Assessment

Task 1 - NDI Assessment State-of-the-art NDI methods were evaluated using the expertise of the program NDI consultant, Dr. L. Adler of Ohio State University, to select a new NDI technique for determining the soundness of the cast plates and components tested during the program. Precise knowledge of the size, location, and types of discontinuities in the test castings was essential so that detected defects could be related to radiographic soundness.

Task 2 - Alloy Definition Concurrent with Task 1, the effects of process variables on the durability and damage tolerance (DADT) properties of D357-T6 and B201-T7 were assessed. Screening tests were conducted during the Screening portion of this task to identify the process variables that provided the optimum balance of tensile and DADT properties for each of the two alloys. Under the Verification portion of this task additional castings were then made using those process variables that provided the optimum properties, and the DADT properties were comprehensively characterized. This verification material will become the baseline for the remainder of the program.

Task 3 - Effects of Defects on DADT Properties The effects of discontinuities and metallurgical features (microstructure) on the DADT properties of D357-T6 are being determined. Because the emphasis of this program is on D357-T6, only the effect of microstructure will be determined for B201-T7.

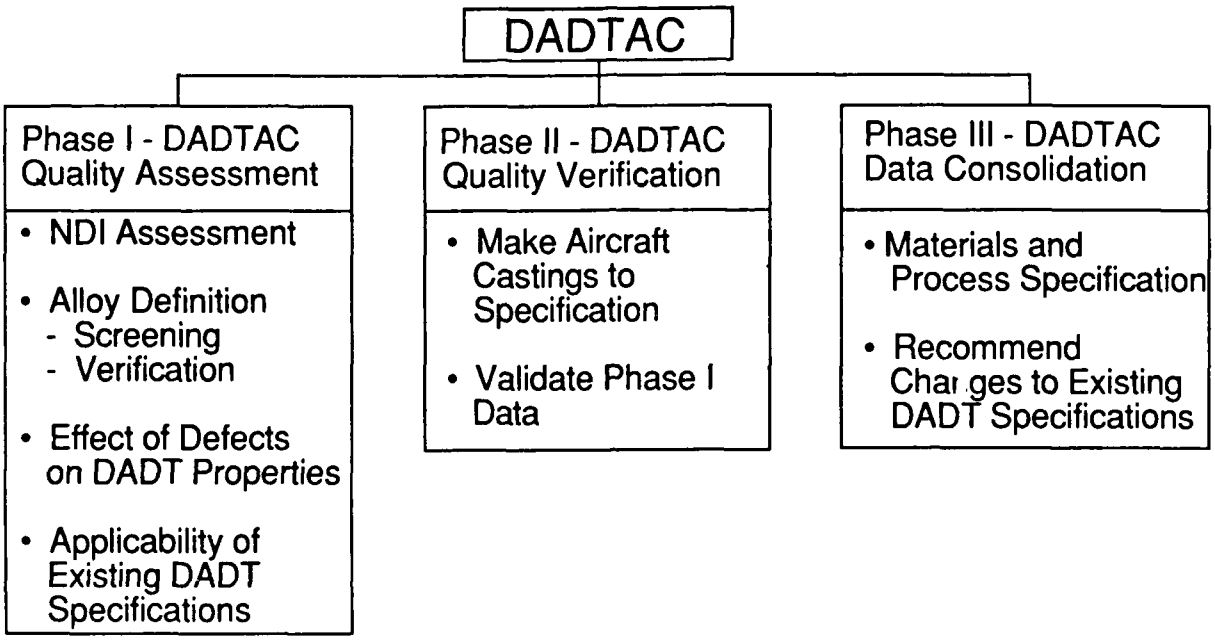

Figure 1. Program Outline

Task 4 - Applicability of Existing DADT Specifications The applicability of the MIL-A-83444 and MIL-A-87221 specifications to D357-T6 and B201-T7 aluminum castings will be assessed, based on the data generated in Tasks 1-3.

Phase II - DADT of Aluminum Castings Quality Verification

During Phase II, the DADT properties obtained during the Phase I, Task 2 verification testing will be confirmed by testing coupons removed from a cast aircraft component. After considering several existing castings, one that meets the program requirements will be chosen. Four castings of the selected design will be produced based on the processing and material specification guidelines from Phase I, and will then be subjected to NDI and DADT property evaluations. The results will be compared with those obtained during Phase I to ensure that the process requirements can be scaled-up from small cast plates to a large aircraft casting.

Phase III - DADTAC Program Data Consolidation

In Phase III, the results of Phases I and II will be consolidated. Material and process specifications, including any necessary silicon modification and NDI requirements, will be prepared for use in producing premium quality aluminum castings for primary aircraft structure. Necessary modifications to existing damage tolerance specifications, such as MIL-A-83444 and MIL-A-87221, will be identified and pursued as required.

SECTION 4
EXPERIMENTAL PROCEDURES

4.1 PRODUCTION OF CASTINGS

D357-T6 and B201-T7 plates were cast by Hitchcock Industries, Fansteel Wellman Dynamics, and Alcoa according to specifications derived from the screening evaluations reported in the first interim report [1]. The specifications were based on the process variables that provided the best overall balance of tensile and DADT properties. The use of three foundries to produce material to the same specification enabled the property variations typical of the casting industry to be determined. The D357-T6 results for one of the three foundries were not available in time for inclusion in this report. The foundries are referred to as Foundries A, B, or C, and do not correspond to the order listed above.

Plates that were 16 inches x 6 inches x 1.25-inch-thick were used for the verification evaluations of Task 2 covered in this report. This plate thickness enabled fracture toughness specimens of a valid thickness to be obtained. However, a limited number of plates of the same thickness used previously in the screening evaluations of Task 2 [1] were also made and evaluated to (a) assure that the verification material properties were similar to those obtained from the best screening task plates and (b) to obtain an indication of the effect of thickness on tensile properties.

The specifications given to the foundries, which were structured to be similar to the AMS 4241 [2] and 4242 [3] aluminum casting alloy specifications for D357-T6 and B201-T7, respectively, are outlined in the following sections. Key mechanical and microstructural properties were specified, but the foundries were given the freedom to select the production methods that would best enable them to produce plates with the required properties. The plates were designated in all areas.

4.1.1 D357-T6

Screening evaluation data [1] indicated that there was no conflict in the requirements for optimizing tensile and DADT properties. Therefore, the AMS 4241 composition specification [2] was used, Table 1, with the addition of strontium as a silicon modifier, which was shown in the screening evaluations [1] to improve mechanical properties, particularly the NTS/YS ratio (an indicator of toughness) and ductility. Although Sr was used during the screening evaluation, one foundry preferred to use sodium for the verification plates because previous experience indicated that it provided benefits at the foundry without impairing the modification process. The other foundry used Sr.

A maximum DAS of 0.0024 inch throughout the plates was specified. This DAS value was selected based on the results of the screening evaluations; plates with a more rapid solidification rate (DAS of 0.0024 inch or less) had higher ultimate tensile strengths (UTS), ductilities, notched tensile strengths, NTS/YS ratios, and fatigue lives than those with a slower cooling rate (larger average DAS).

Each foundry produced two plates of the same size as the screening plates (12 inches x 6 inches x 0.75 inch) and eight larger plates (16 inches x 6 inches x 1.25 inch). The smaller plates, which were the same size as those used in the screening evaluation portion of Task 2, were tested to assure that the properties of the optimally-produced screening material could be reproduced using the verification material specifications. Because castings are often quenched in a glycol/water solution to reduce distortion (by reducing the cooling rate) of complex parts and/or those that have significant thickness variations, three of the eight large plates were quenched in a room temperature glycol (25%)/water solution (GQ); the remaining plates were quenched in room temperature water (WQ). The rigging system and

TABLE 1. COMPOSITION SPECIFICATION[1] FOR THE D357 VERIFICATION PLATES

Element	Range (wt %)	
	Min.	Max.
Silicon	6.5	7.5
Magnesium	0.55	0.6
Titanium	0.10	0.20
Beryllium	0.04	0.07
Strontium (2)	0.008	0.014
Sodium (2)	0.002	0.012
Iron	-	0.12
Manganese	-	0.10
Others, each	-	0.05
Others, total	-	0.15
Aluminum	Balance	

(1) AMS 4241 plus Si modifier

(2) Sr <u>or</u> Na was used, not both.

aging treatments were the same for the GQ and WQ plates, allowing the effect of quench medium on DADT properties to be determined.

The specified minimum tensile properties were based on the results obtained during the screening evaluations and were identical to the AMS 4241 specification for designated areas, as follows:

Ultimate tensile strength	- 50 ksi
Yield strength at 0.2% offset	- 40 ksi
Elongation	- 3%

The foundries selected their preferred aging procedures to meet the mechanical property requirements.

A flat vacuum density test result was specified to assure that the melt hydrogen gas content, which influences the amount of porosity in the final casting, was minimized.

No weld repair was allowed, and each plate was required to be Grade B or better by 1% sensitivity radiography according to MIL-STD-2175.

4.1.1.1 D357 Castings

The rigging system for the 0.75-inch-thick plates was described in an earlier report [1]. The rigging systems and the heat treatment procedures used by Foundries A and B for the 1.25-inch-thick D357-T6 plates are described below.

Foundry A

The rigging, shown in Figure 2, consisted of a tapered down sprue leading into a pouring well and runner system which fed the vertical mold cavity. Three 1.25-inch-thick copper chills were

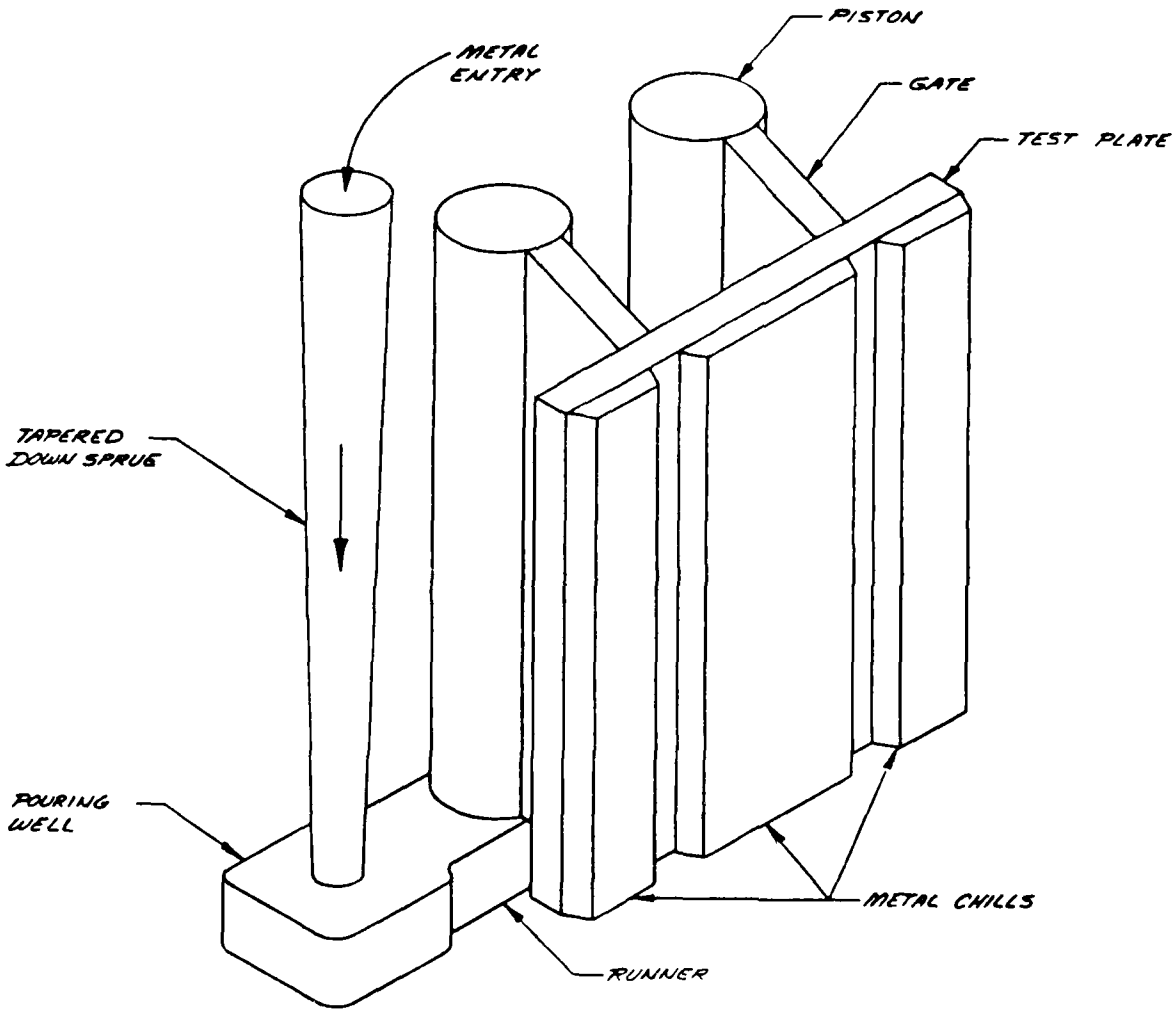

Figure 2. Rigging System Used by Foundry A to Produce D357 Plates.

used, and a fiberglass screen was placed between the pouring well and runner to trap foreign material.

The plates were solution heat treated for 15 hours at 1015F in a drop bottom furnace. The temperature was controlled to within +5F and -10F. The plates were quenched in room temperature water or a 25% glycol-water solution, and were artificially aged at 335±5F for 6 hours.

Foundry B

The rigging for the plates produced by Foundry B is shown in Figure 3. Eight 2-inch by 2-inch by 1.5-inch-thick iron chills placed end on end were used in the center of the horizontal cope, and one 3-inch by 3-inch by 16-inch-long copper chill was used in the drag to obtain directional and rapid solidification. Eight insulated risers spaced at approximately 4-inch intervals were used to feed the casting during solidification. The mold cavity was gravity fed through an insulated gating system which contained ceramic filters to trap foreign material.

The plates were solution heat treated at 1010±5F for 24 hours and quenched in room temperature water or a 25% glycol-water solution. The plates were then artificially aged at 315±5F for 13.5 hours.

4.1.2 B201-T7

Similar to D357-T6, the screening evaluation data showed that there was no conflict in the requirements for optimizing tensile and DADT properties. Consequently, the composition specified in AMS 4242 (Table 2) [3] was used for the verification plates. Each foundry produced two 0.75-inch-thick plates and five 1.25-inch-thick plates and selected their preferred aging treatment to meet the mechanical property requirements. All areas of the plates required designated properties and all of the

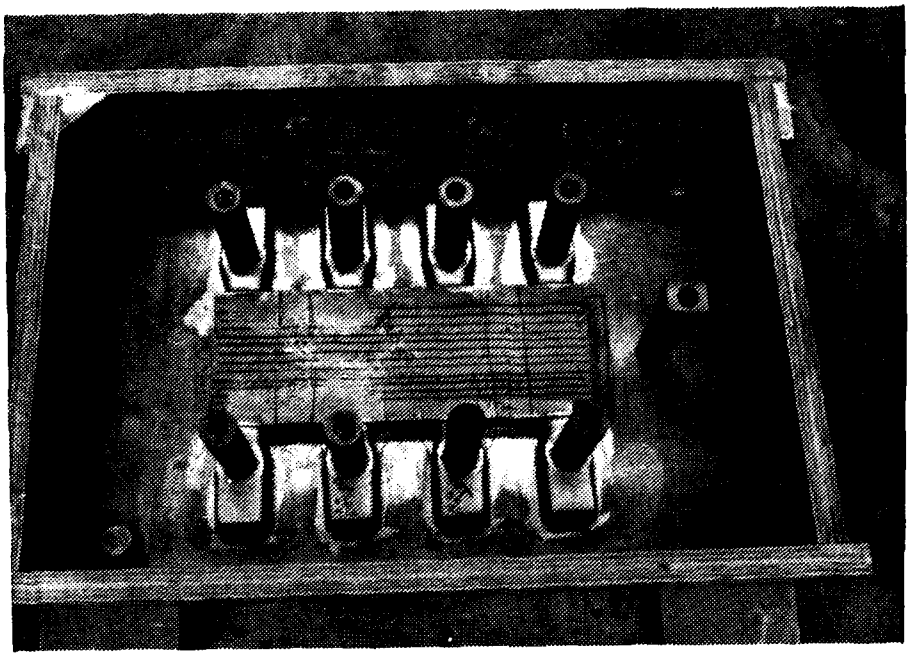

a. Cope Side of Casting.

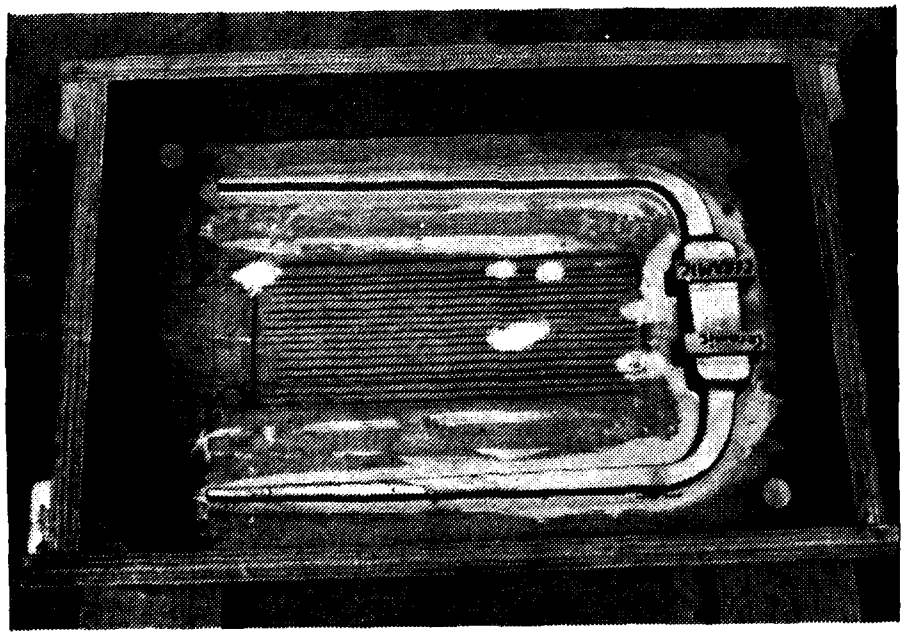

b. Runner and Filter System.

Figure 3. Rigging System Used by Foundry B to Produce D357 Plates.

TABLE 2. COMPOSITION SPECIFICATION[1] FOR THE B201 VERIFICATION PLATES.

Element	Range (wt %)	
	Min.	Max.
Copper	4.50	5.0
Silver	0.40	0.8
Maganese	0.20	0.50
Magnesium	0.20	0.30
Titanium	0.15	0.35
Iron	-	0.05
Silicon	-	0.05
Others, each	-	0.05
Others, total	-	0.15
Aluminum	Balance	

[1] AMS 4242

plates were quenched in room temperature water. A flat vacuum density test result was required. To minimize microshrinkage, which may have a deleterious effect on fatigue life, all B201 plates were HIPed. HIPing consisted of step-heating the as-cast plates to 950F and holding for 3 hours in an inert gas atmosphere at 15,000 psi.

The specified minimum tensile properties were based on the results obtained during the screening evaluations and were identical to the AMS 4242 specification requirements for designated areas, as follows:

Ultimate tensile strength	- 60 ksi
Yield strength at 0.2% offset	- 50 ksi
Elongation	- 3%

Similar to D357-T6, weld repairs were not allowed, and each plate was required to be of a Grade B or better radiographic quality (1% sensitivity).

4.1.2.1 B201 Castings

Similar to the D357 plates, each foundry designed its own rigging system and chose the solution heat treat and aging parameters they thought best to achieve the T7 temper with the required mechanical properties. The rigging system for the 0.75-inch-thick plates was described in an earlier report [1]. The rigging systems and heat treatment procedures used by Foundries A, B, and C for the 1.25-inch-thick plates are described below.

Foundry A

The rigging for plates produced by Foundry A was the same as that used for the D357 plates (Figure 2).

The plates were loaded in a furnace below 500F and solution heat treated as follows:

2 hours at 940±10F
2 hours at 960±10F
16 hours at 980±10F

The plates were then quenched in room temperature water and artificially aged for 5 hours at 380±5F.

Foundry B

The rigging for the plates produced by Foundry B was similar to that shown in Figure 3 except that no chills were used in the cope. One 2-inch by 3-inch by 16-inch-long copper chill was used in the drag to obtain directional solidification. Eight insulated risers spaced at approximately 4-inch intervals were used to feed the casting during solidification. The mold cavity was gravity fed through an insulated gating system which contained ceramic filters to trap foreign material.

The plates were loaded into a furnace below 500F and solution heat treated and quenched as follows:

2 hours at 940±10F
2 hours at 950±10F
16 hours at 980±10F

The plates were then quenched in room temperature water and aged for 8 hours at 360±5F.

Foundry C

The rigging for the plates produced by Foundry C is shown in Figure 4. Two 2.5-inch by 2.5-inch by 8-inch cast iron chills placed end on end were used in the cope, and one 2-inch by 4-inch

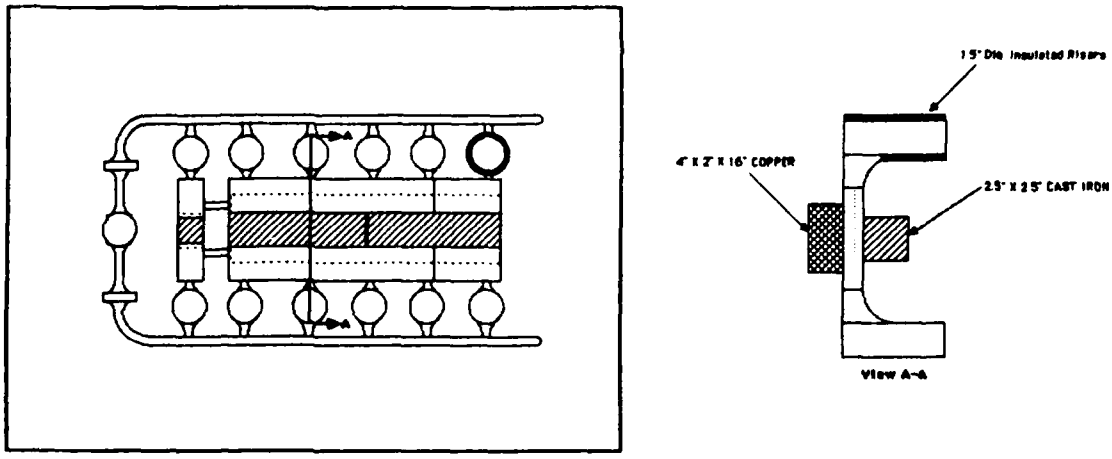

Figure 4. Rigging System Used by Foundry C to Produce B201 Plates.

by 16-inch-long chill was used in the drag to obtain directional solidification. Ten 1.5-inch-diameter insulated risers spaced at approximately 4-inch intervals were used to feed the casting during solidification. The mold cavity was gravity fed through the gating system, which contained ceramic foam filters to trap foreign material.

The plates were loaded into a furnace below 500F and solution heat treated as follows:

2 hours at 920±10F
2 hours at 950±10F
2 hours at 970±10F
16 hours at 980±10F

The plates were quenched into room temperature water and then naturally aged at room temperature for 24 hours, followed by artificial aging at 360±5F for 8 hours.

4.2 TEST PROCEDURES

The 1.25-inch-thick plates used for the verification evaluations were comprehensively evaluated using the tests shown in Table 3, and were radiographically inspected to assure all materials were Grade B or better. The DADT test specimens were excised randomly from the 1.25-inch-thick plates to determine the between-plate and foundry-to-foundry mechanical property variability.

For the 0.75-inch-thick verification plates, only tensile and notched tensile tests were conducted. The results were compared with the screening test data to assure that the properties obtained from the optimized screening evaluation plates [1] could be reproduced in the verification plates.

TABLE 3. VERIFICATION TESTS FOR D357-T6 AND B201-T7.

Test	Specification	Number of Tests		
		D357-T6		B201-T7
		Water Quench	Glycol Quench	Water Quench
Tensile	ASTM B557	30	10	30
Notched Tensile	ASTM E602	30	10	30
Fracture Toughness	ASTM B646(1)	6	3	6
Constant Amplitude Fatigue Crack Growth	ASTM E647	6	3	6
Stress-Life Fatigue	ASTM E466	12	6	12
Stress Corrosion	ASTM G47	0	0	3
Strain-Life Fatigue	ASTM E606(2) and E466	12	0	12
Metallography	ASTM E112	15	6	15
Chemical Analysis	NA	15	6	15

(1) In addition to the ASTM 646 standard test, short bar testing was performed using the method currently under review by ASTM.
(2) A new specification is under review by ASTM.

The composition of each plate was determined using Inductively Coupled Plasma (ICP) analysis to confirm the foundry melt results. The DAS of the D357 plates was measured using a line intercept method [4] and the silicon particle morphology was evaluated using an Omnicon 3500 image analyzer. Specimens were excised from random locations throughout the plates.

4.3 EQUIVALENT INITIAL FLAW SIZE ANALYSIS

Durability and damage tolerance analysis requirements for aircraft structure are defined in MIL-A-83444 and MIL-A-87221. For damage tolerance analysis of wrought alloys, the presence of a flaw is assumed so that defects that may occur in critical areas of a part during manufacturing are accounted for. Castings contain inherent flaws such as microporosity, microshrinkage, or foreign material that may not be detectable by normal NDI methods. A limited amount of these defects is acceptable in premium quality aluminum castings for aerospace applications. An equivalent initial flaw size (EIFS) must be determined for castings to account for these inherent flaws. The EIFS of D357 and B201 was determined from the Task 2 (verification) fatigue data using a method developed previously under a Northrop IR&D Program [5]. The methodology for determining the EIFS and how it may be applied to both durability and damage tolerance analyses are summarized below. The damage tolerance analysis is included in Section 5 of this report. The durability analysis is scheduled to be concluded later in the program.

4.3.1 Determination of Equivalent Initial Flaw Size

Stress-life fatigue results for smooth round-bar specimens (K_t = 1.0) were used to obtain an estimate of the inherent material EIFS. The value of EIFS (a_o), which initiates a crack in a smooth round bar fatigue specimen, is based on the following relationship [5].

$$a_o = \left\{ a_i^{(1-m/2)} - (1-m/2)C(\beta\Delta S\sqrt{\pi/Q})^m N_i \right\}^{1/(1-m/2)} \qquad \text{Eq. 1}$$

where

a_i = a selected flaw size defining initiation which is close to, but in excess of a_o by at least 0.01 inch.

m & C = the slope and intercept, respectively, of the Paris law equation representing the da/dn vs ΔK plot. For this analysis, the da/dn test must be run at the same stress ratio as the stress-life fatigue tests.

β = the stress intensity correction factor for a semicircular surface flaw of a depth equal to the average of a_o and a_i.

ΔS = the elastic stress range of the fatigue specimen.

N_i = Number of cycles for the fatigue crack to grow to a_i from a_o.

Q = a crack shape factor, equal to $2.464-0.212(S_{max}/\sigma_y)^2$.

where S_{max} = the maximum fatigue stress.

σ_y = yield strength.

The value of N_i is determined from the number of cycles to failure using the following relationship:

$$(N_f/N_i) = 1 + \frac{(a_i + a_o)^{m/2}}{(a_i - a_o)} \sum_{a=a_i}^{a_c} \left\{ \frac{\Delta a}{\left(\frac{\beta\bar{a}}{\beta_i}\right)^m (2\bar{a})^{m/2}} \right\} \qquad \text{Eq. 2}$$

where: $\bar{a}$ = the crack length at the midpoint of the assumed interval, Δa.

$\beta_{\bar{a}}$ = the stress intensity correction factor at crack length $\bar{a}$.

The EIFS solution involves an interpolation between Equations 1 and 2 because each one contains a_o. However, an adequate convergence occurs within seven or eight iterations depending on the initial value of a_i assumed.

4.3.2 Application to Durability Analysis

The durability analysis will be performed using the Northrop sequence crack initiation program, LOOPIN8 [6] using data generated from round bar strain-life fatigue test specimens. These specimens have the same general geometry as those used to obtain the EIFS (Section 4.3.1).

Using the average EIFS obtained as described in Section 4.3.1, the ratio between N_i and N_f for each alloy can be derived from Equation 2 for a selected value of initiation flaw size (a_i). Hence, the failure lives obtained during the strain-life tests can be converted to the cycles required to initiate a crack of the selected size. Using these converted data, the LOOPIN8 program is then used to predict the life to initiate a crack from the material EIFS (a_o) to the predefined initiation flaw size (a_i).

4.3.3 Application to Damage Tolerance Analysis

Damage tolerance analysis is based on the assumption that crack growth starts from a "rogue" flaw. For wrought alloys, the size of this flaw is generally defined [7] as a 0.050 inch corner flaw at the edge of a hole. Reductions in the assumed value of this flaw are negotiable between the supplier and the customer based on a demonstration of manufacturing quality. However, if the basic quality of the material is such that similar or greater rogue flaws can exist regardless of the care taken to produce the

finished article, then the upper bound of the inherent material equivalent initial flaw size becomes the limiting design factor.

The upper bound for the castings was derived from the EIFS distribution obtained from smooth round bar fatigue test results using a "sudden-death" analysis, as described below.

Sudden-Death Analysis

Sudden-death testing [8] is a method that can be used for determining the upper bound defect size for the general population based on the fatigue life results for specimens that contain random distributions of casting defects. Crack initiation will usually occur at the largest defect located at or near the surface of the gauge section of the specimen. The failure of the specimen can be assumed to be the "sudden-death" failure of the set of defects contained within the surface volume of the specimen. The largest defect is represented by the shortest fatigue life.

The smooth round bar fatigue specimens used in the DADTAC program had a 1.6-inch-long by 0.50-inch-diameter gauge section. The volume of material in the critical initiation zone of these specimens is equivalent to that obtained in a similar depth of material at the edge of approximately 70 0.25-inch-diameter holes drilled through a 0.25-inch-thickness. This estimate is based on an assumption that the critical high stress concentration region for a hole extends twenty degrees either side of the hole axis aligned normal to the primary load direction. This is considered to be a conservative assumption as a more localized stress concentration would tend to increase the number of holes represented by the smooth bar specimen.

According to the theory of ranking [8], the lowest value in a set of 70 specimens clusters about the 1% probability level of the general population. If the lowest life represents the

highest equivalent initial flaw size in each set of 70, then the EIFS values obtained from an analysis of the round bar tests will be clustered about the 99% probability level of the EIFS values obtained for a typical defect population.

The ranked results are analyzed assuming a Weibull distribution to obtain the median and upper 95% confidence limit statistics of the "sudden death" population. The median and upper 95% confidence limit of the general population are obtained by translating the "sudden death" median line and confidence limit upward until the Weibull median value of the "sudden death" line coincides with the 99% probability value.

EIFS values for castings obtained from different vendors were grouped using variance analysis [9]. An estimate of the maximum inherent material rogue flaw size was obtained from the 99.9% probability and 95% confidence value read from the above derived general population distribution. If this value exceeds the current requirements of MIL-A-83444 it indicates that the basic material quality is more critical for the castings evaluated under the DADTAC program than the upper flaw sizes currently assumed for wrought alloys based on manufacturing quality. A value less than the current MIL-A-83444 specification requirement would indicate that castings can be considered for use in a damage tolerant design by applying the same criteria used for wrought alloys.

SECTION 5
RESULTS AND DISCUSSION

The overall objective of the verification subtask was to determine the DADT properties of D357-T6 and B201-T7 made to the specifications developed in the screening subtask. The results for the two alloys are described in the following subsections.

5.1 D357-T6 RESULTS

The main emphasis for D357 was to evaluate cast plates that were quenched in room temperature water. However, a few D357 plates were quenched in glycol (GQ) to determine if the quench medium significantly influenced the mechanical properties. All other process parameters for the GQ plates were the same as for the water-quenched (WQ) plates.

For the WQ plates, only those that fully met the specified microstructural and tensile properties as well as radiographic quality and chemical composition, were used for evaluating DADT properties. To fully evaluate the effect of the quench, all of the GQ plate test results were compared with data from the WQ plates. However, only data from those GQ plates which fully met all the specification requirements were included in the subsequent DADT analyses (e.g. EIFS).

All the WQ and GQ D357-T6 plates from Foundry A met the specification requirements. The DADT test specimens, therefore, were excised from these plates at random locations. For Foundry B, two WQ plates did not meet the tensile property requirements; both had one low elongation value (<3%) out of the two tensile specimens tested from each plate. Therefore, only the remaining three plates were used for the DADT characterization described in this section. The evaluations for Foundry C material were not complete at the time this report was prepared.

5.1.1 Composition

A combined total of sixteen plates (1.25-inch- and 0.75-inch-thick) cast from ten different melts by two foundries were used for the verification evaluations. The composition of each of these melts and the specification ranges for each element are listed in Table 4. The compositions were within the range specified from the screening subtask of this program (Table 1). The melt analyses were confirmed by ICP chemical analyses on samples taken from the plates.

5.1.2 Microstructure

The microstructure of the D357-T6 plates was characterized using optical, transmission and scanning transmission electron microscopy (TEM and STEM), and scanning electron microscopy (SEM). The DAS and silicon particle morphology of each plate were determined. A typical optical micrograph of D357-T6 is shown in Figure 5.

The DAS of specimens taken from various locations throughout the plates ranged from 0.0008 inch to 0.0020 inch, which is within the specification requirement ($\leq$0.0024 inch).

The average DAS values, as well as the Si particle area, spacing, and aspect ratio for WQ and GQ material from both foundries are listed in Table 5, along with a comparison to the corresponding data obtained previously for the screening material. The DAS for material from the two foundries was similar, with all values being below the specification maximum of 0.0024 inch. The average DAS of the verification material was slightly less than that of the screening material. The average DAS for the GQ plates from both foundries was less than that for the WQ material. The GQ and WQ plates were made to the same specification using identical processing conditions except for the quench medium. There was no variation in chill or mold materials which would affect the DAS. Therefore, the consistent

TABLE 4. D357 VERIFICATION MATERIAL MELT COMPOSITIONS.

COMPOSITION (wt %)								
Fe	Si	Mg	Ti	Mn	Be	Na	Sr	Al
0.03	7.03	0.6	0.12	0.00	0.050	0.002	-	Bal.
0.03	6.99	0.6	0.11	0.00	0.070	0.003	-	Bal.
0.03	7.27	0.6	0.10	0.00	0.060	0.009	-	Bal.
0.04	7.37	0.6	0.11	0.00	0.050	0.012	-	Bal.
0.11	6.67	0.6	0.16	0.01	0.061	-	0.008	Bal.
0.10	7.35	0.6	0.15	0.01	0.070	-	0.014	Bal.
0.11	6.80	0.6	0.17	0.01	0.059	-	0.011	Bal.
0.10	7.07	0.6	0.15	0.01	0.069	-	0.014	Bal.
0.11	7.20	0.6	0.16	0.01	0.070	-	0.007	Bal.
0.10	7.07	0.6	0.15	0.01	0.069	-	0.014	Bal.
AMS 4241 Specification Range								
<0.12	6.5-7.5	0.55-0.6	0.10-0.20	<0.1	0.04-0.07	*	*	Bal.

* Not specified in AMS 4241; however, those amounts used are within the 0.05 wt. % limit set for "other" elements.

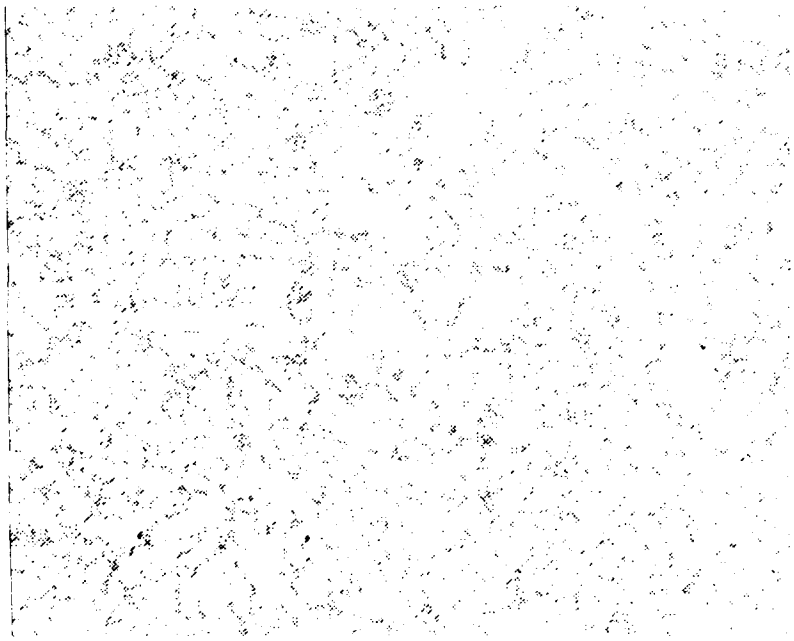

50X As polished

Figure 5. Typical D357-T6 Microstructure.

TABLE 5. D357 DAS AND Si PARTICLE DATA.

Foundry	Quench	DAS (inch)	Si Particle Morphology Area (μm^2)	Spacing (μm)	Aspect Ratio	% Porosity
A	Water	0.0012	16	38	1.6	0
	Glycol	0.0010	12	36	1.6	0
B	Water	0.0018	18	44	1.6	0.083
	Glycol	0.0013	23	40	1.6	0
Average	Water	0.0015	14	41	1.6	0.042
	Glycol	0.0011	18	38	1.6	0
Average of Screening Data [1]		0.0016	20	36	1.8	0.023

difference in the DAS for the GQ and WQ plates is considered to be coincidental and not a result of processing differences.

The silicon particle data for the verification material from the two foundries were also similar, and were similar to those obtained previously for the screening material. The percent porosity, which was determined using the optical metallography specimens, was low for all of the verification plates, as it was in the screening plates. An additional indication of the amount of gas porosity was obtained by measuring the residual hydrogen present in samples of the cast material. The average hydrogen content of samples from both foundries was 0.65 ppm.

The microstructure of randomly selected samples was evaluated using SEM, TEM, STEM, SAD patterns, and EDX analyses. Four different phases were observed, although the exact stoichiometry of three could not be determined.

A typical SEM micrograph of D357-T6, Figure 6, shows three phase morphologies in addition to the aluminum matrix. Using EDX analyses, the shapes identified by Numbers 1 and 2 were determined to be Al-Fe, but the stoichiometry could not be determined. The phase identified by Number 3 was determined by EDXA to be Si. Smaller Si particles were also observed in the TEM micrograph, Figure 7. An X-ray map of the microstructure confirmed that these particles were Si. Long needle-shaped particles were also observed in the microstructure of Figure 8, and were shown by X-ray mapping to contain Ti. Mg and Fe X-ray maps of this microstructure were also generated, but neither element was detected. A closer examination of the Ti-containing needles was conducted to determine their stoichiometry. Figures 9a and b show a typical needle and its SAD pattern, respectively. Examination of the pattern, as well as two others obtained at different orientations, did not reveal the composition or stoichiometry of the phase. Another phase is also seen in

Figure 6. Backscatter SEM Micrograph of D357-T6.

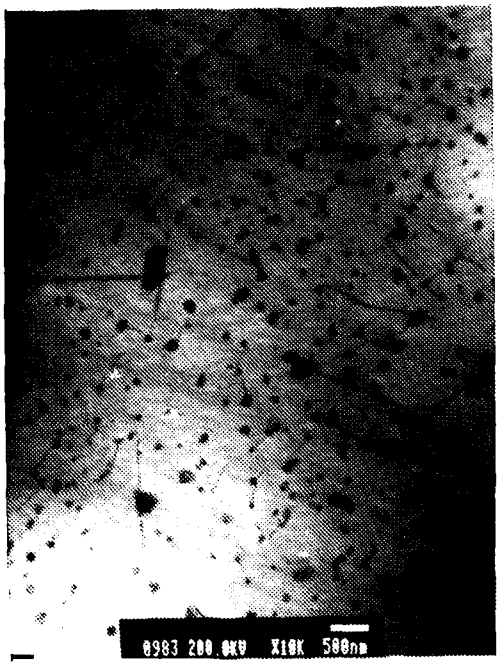

Figure 7. TEM Micrograph of D357-T6 Showing Si Particles.

Figure 8. TEM Micrograph of D357-T6 Showing a Needle-Shaped Phase Containing Ti.

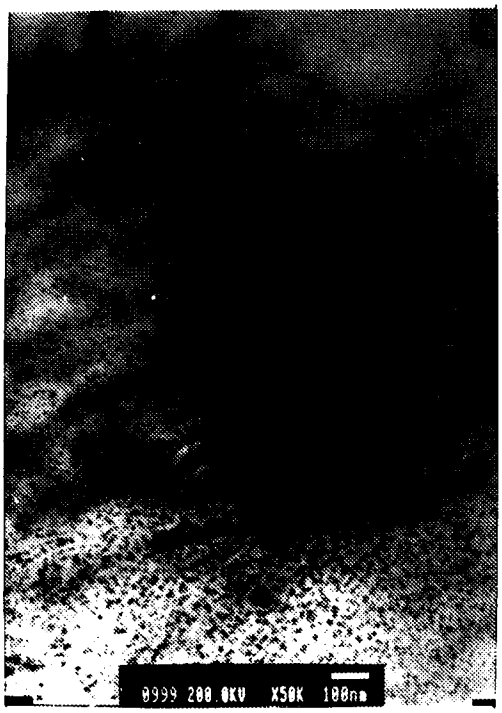

Figure 9a. TEM Micrograph of D357-T6 Showing a Needle-Shaped Particle Containing Ti and Smaller Mg_2Si Particles.

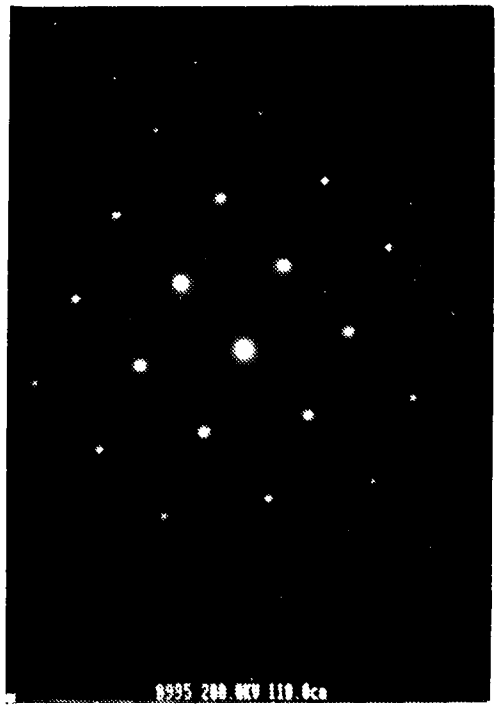

Figure 9b. Selected Area Diffraction Pattern of the Needle Phase of Figure 9a.

Figure 9a, which was identified by EDXA to be the main strengthening phase Mg_2Si.

Sodium was used to modify the as-cast microstructure of the specimen that was examined in the TEM. However, X-ray mapping and diffraction patterns of various areas of the microstructure failed to locate Na. Some controversy exists about the exact modification mechanism caused by Na. However, one theory [10] is that modification is accomplished through an interaction between Na and P, an impurity element. In the absence of Na, P forms AlP, which promotes the formation of large Si particles. When Na is added, the compound NaP is formed, which suppresses this tendency, resulting in a finer microstructure.

5.1.3 Tensile Properties

The tensile properties of D357-T6 plates from Foundries A and B are shown in Table 6. Tests were conducted on both water- and glycol-quenched material from the 1.25-inch-thick plates. A limited number of tensile tests were also conducted on the 0.75-inch-thick plates (water-quenched only). These smaller plates were evaluated to assure that those properties obtained for the optimized material during the screening evaluations could be reproduced in plates of the same size produced to the AMS 4241 specification. The combined average tensile properties for the 0.75-inch-thick verification plates from Foundries A and B were 53.6 ksi ultimate strength, 45.3 ksi yield strength, and 5.9 percent elongation. These values were similar to the results from the screening tests, i.e. 51.4 ksi, 43.4 ksi, and 5.1, respectively.

The average and minimum tensile properties for the 1.25-inch-thick water-quenched material from Foundry A (54/45/5.9) were slightly higher than those from Foundry B (52/45/4.5). All of the individual test specimens from the Foundry A plates met the 50/40/3 tensile property requirements. Two Foundry B plates

TABLE 6. TENSILE PROPERTIES OF THE 1.25-INCH-THICK, WATER- AND GLYCOL-QUENCHED* D357-T6 PLATES.

Foundry	Quench** Medium	UTS (ksi) Avg.	UTS (ksi) Range	YS (ksi) Avg.	YS (ksi) Range	El (%) Avg.	El (%) Range
A	Water	54	51-55	45	44-47	5.9	3.5-8.5
	Glycol	53	51-55	43	42-44	6.6	5.5-9.0
B	Water	52	50-53	45	44-46	4.5	3.0-5.6
	Glycol	49	48-50	42	41-43	3.4	2.5-4.3
Average	Water	53		45		5.2	
	Glycol	51		43		5.0	
Target Min.		50		40		3.0	

*25% Glycol Solution
**Room Temperature

each had one tensile test result that had a percent elongation less than the 3.0% minimum requirement. Subsequent DADT evaluations of material from Foundry B were conducted only on those plates that fully met the tensile property specification requirements. The tensile property data for Foundry B material shown in Table 6 include only those WQ plates that were within the specification.

The average and minimum tensile property data for GQ plates from both foundries are also shown in Table 6. Strength levels are in general slightly lower than those for the WQ material. The reduction in strength is probably associated with a lower level of Mg remaining in solution following the quench, resulting in less Mg_2Si, the strengthening phase, following artificial aging. Two of 12 elongation values for the GQ plates were below the 3.0 percent minimum.

5.1.4 Fatigue Properties

5.1.4.1 Smooth Stress-Life

The stress-life data for D357-T6 (k_t=1.0) from Foundries A and B are shown in Figure 10 along with a comparison to 7075-T73 [11], a wrought alloy commonly used in fatigue critical aircraft applications. The fatigue lives of material from Foundry A are longer than those for Foundry B for a given stress level. The fatigue lives of the GQ and WQ material are essentially the same. The average fatigue life of D357-T6 is less than that of 7075-T73, and is presumably due to lower D357-T6 strength and the larger size of the inherent defects found in castings, which will tend to reduce the initiation life, as discussed in Section 5.1.4.4.

5.1.4.2 Smooth Strain-Life

The strain-life data are shown in Figure 11 as log strain amplitude vs. log of the number of cycles to failure (N_f).

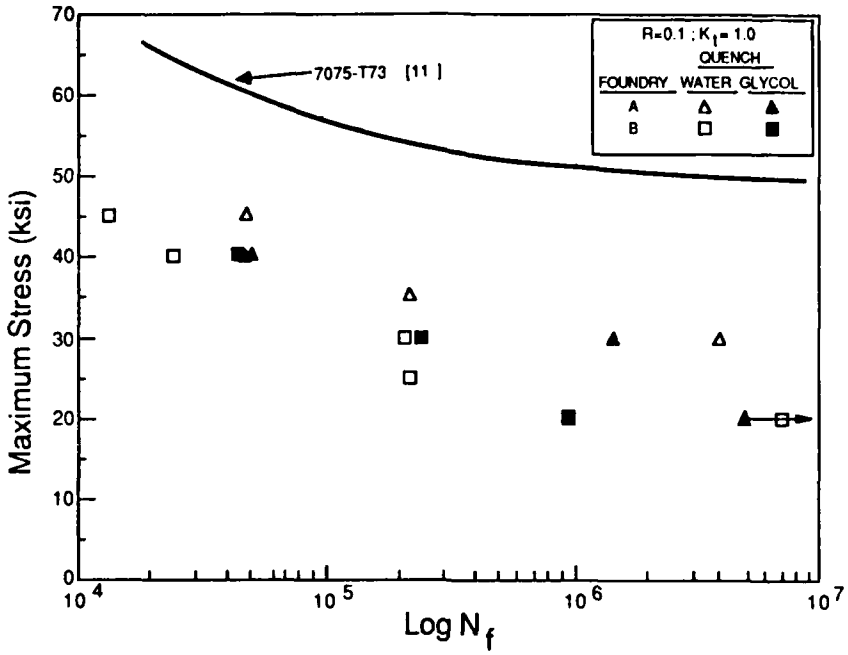

Figure 10. D357-T6 Stress-Life Fatigue Data.

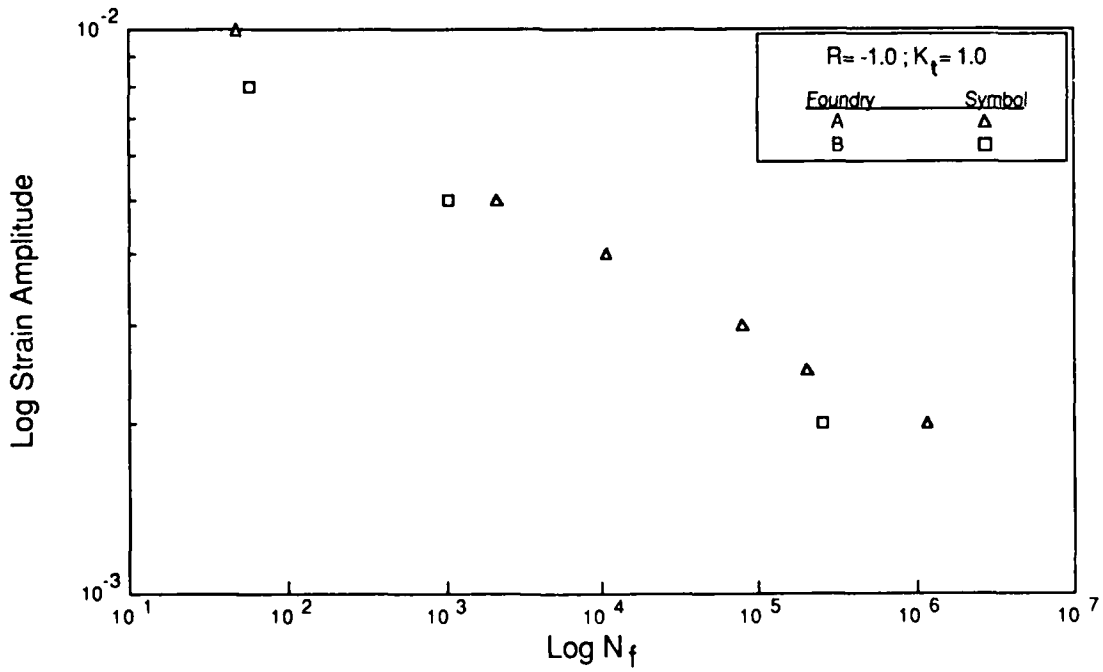

Figure 11. D357-T6 Strain-Life Fatigue Data.

The specimens were tested using an R ratio of -1.0, with strain amplitudes ranging from 0.010 to 0.002, which resulted in fatigue lives ranging from approximately 50 to 1,000,000 cycles. These data were generated for use in the durability analysis later in the program (described in Section 4.3.2).

5.1.4.3 Fatigue Crack Growth Rate

The range of constant amplitude fatigue crack growth rate (FCGR) data for WQ and GQ material from Foundries A and B are shown in Figure 12. Also included are data for A357-T6 obtained under a previous Northrop program [12], and 7075-T7351 plate [13]. The DADTAC D357-T6 data are similar to the previous A357-T6 data and are slightly better than that of 7075-T7351. Based on these data, the difference in the total fatigue life between the cast and wrought materials (Figure 10) can be attributed to the ease of crack initiation. Fatigue cracks probably initiate more readily in castings than in wrought material, due to the presence of inherent defects such as dross and/or porosity. Each fatigue life specimen was fractographically examined to determine the crack initiation site. Out of 12 specimens examined, 11 initiated a fatigue crack from a defect located at or near the surface. No clearly defined defect was associated with the fatigue crack initiation of the twelfth specimen. The results are shown in Table 7. All of the defects were porosity and/or dross. Typical sites are shown in Figures 13a and b.

5.1.5 Fracture Toughness

The fracture toughness data for WQ and GQ D357-T6 are shown in Table 8. Compact tension, short bar, and NTS/YS tests were conducted. A short bar test specimen was removed from each of the tested compact tension specimens to obtain a direct correlation between the two test methods. Invalid K_Q results

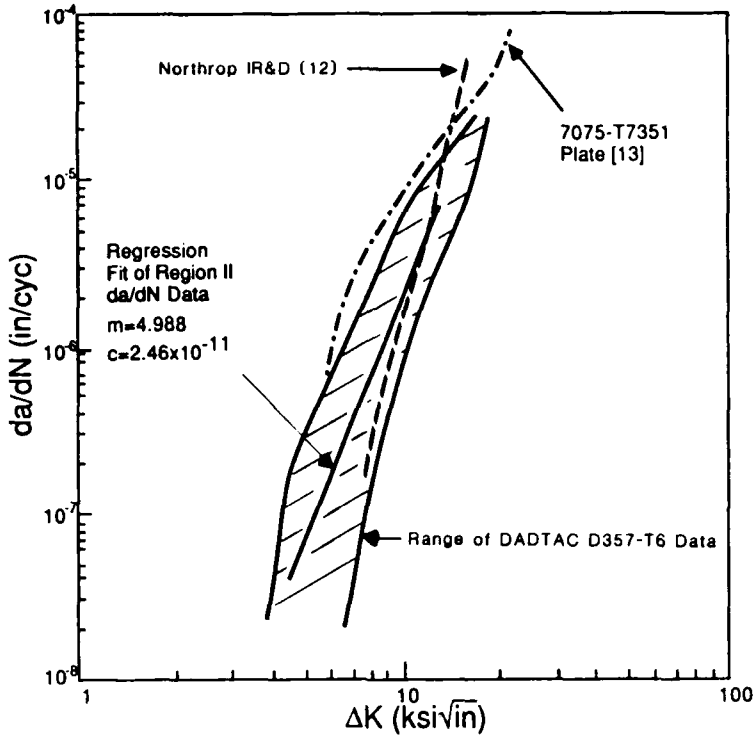

Figure 12. D357-T6 Fatigue Crack Growth Rate Data (R=0.1; lab air).

TABLE 7. FATIGUE CRACK INITIATION SITES FOR D357-T6 FATIGUE SPECIMENS.

Number of Fatigue Specimens With Crack Initiation Site			
Dross	Pore	Both Dross and Pore	Other*
4	4	3	1

*No Observable Defect

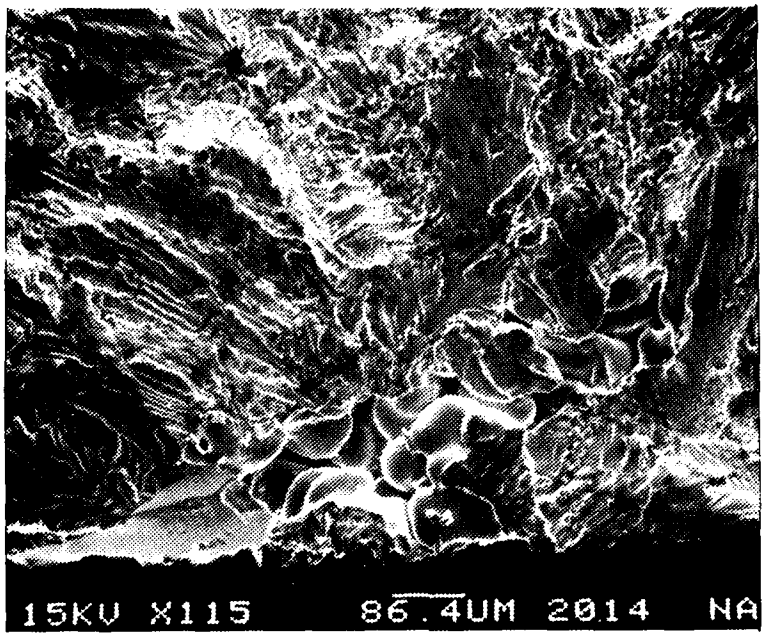

a. SEM Micrograph of a Pore.

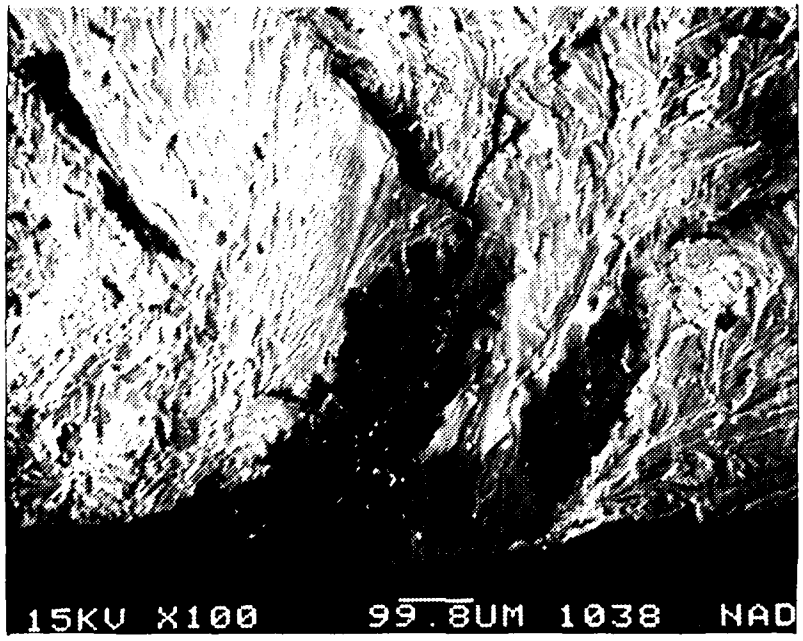

b. Backscatter SEM Micrograph of Foreign Material.

Figure 13. Typical Crack Initiation Sites in D357-T6 Fatigue Specimens.

TABLE 8. AVERAGE D357-T6 FRACTURE TOUGHNESS DATA.

Quench Medium	Fracture Toughness (ksi $\sqrt{in.}$) K_{IC}	K_Q	K_{IV}*	NTS (ksi)	YS (ksi)	NTS/YS
Water	-	24	24	62	45	1.38
Glycol**	22	-	22	57	42	1.36

*Short Bar Test
**25% Glycol Solution

were obtained from the compact tension tests for all the WQ material due to excessive crack front curvature, which is often observed in castings due to residual stresses incurred during quenching. Valid K_{Ic} results were obtained for GQ plates, presumably because of the slower cooling rate associated with the glycol.

For both foundries, an average K_Q of 24 ksi$\sqrt{in}$ was obtained for WQ material by both compact tension and short bar (K_{IV}) test methods. This fracture toughness value corresponded to a NTS/YS ratio of 1.38. The fracture toughness of the GQ material was slightly less than that of the WQ material, 22 ksi$\sqrt{in}$ for both compact tension (K_{IC}) and short bar (K_{IV}) test methods. The average NTS/YS ratio of the GQ material was slightly less than that of the WQ material, 1.36 vs. 1.38. Similar to the WQ material, both foundries had the same average fracture toughness values for the GQ plates.

The ranges of the compact tension and short bar fracture toughness values and their correlations with yield strength are evident by comparing all the test data shown in Figure 14. The fracture toughness ranged from approximately 21 to 26 ksi$\sqrt{in}$, with the lowest values (21 and 22 ksi$\sqrt{in}$, K_{IC}) being obtained for the GQ material. There was no clear correlation between the fracture toughness and yield strength, probably because the yield strength range was relatively narrow. Other work [14] has shown that there is an inverse relationship between fracture toughness and yield strength.

5.1.6 Equivalent Initial Flaw Size Analysis

The method for determining the equivalent initial flaw size was described in Section 4.3.1. The calculated values for individual specimens excised from material from the two foundries are shown in Table 9, along with the corresponding fatigue life and maximum applied stress. Testing of specimens that did not fail after $5x10^6$ cycles was terminated and an EIFS was not

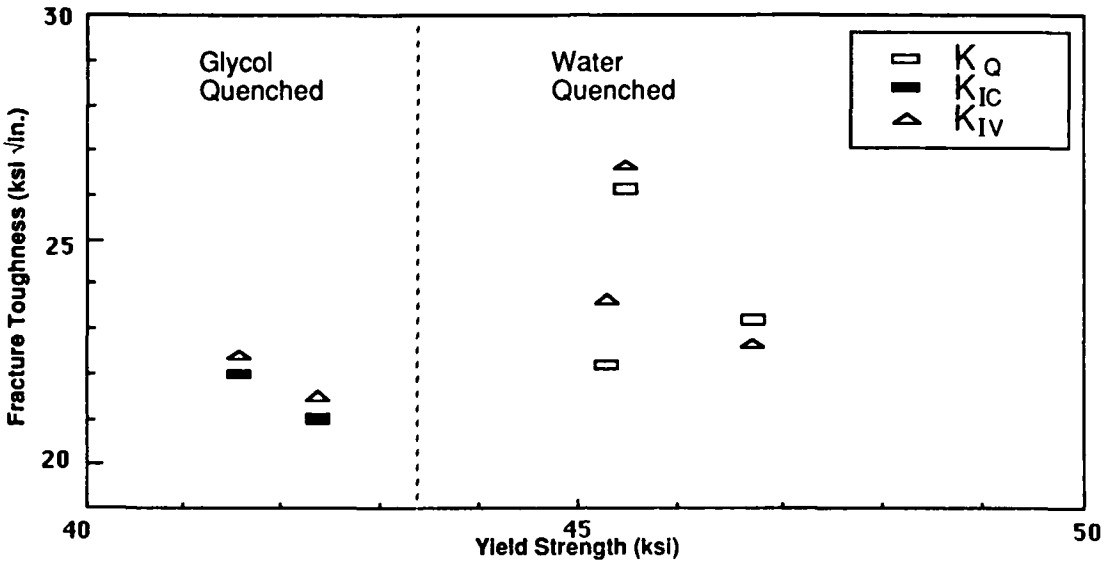

NOTE: All K_{IC} values for glycol - quenched material.
K_{IV} obtained from short bar test.

Figure 14. Relationship Between Fracture Toughness and Yield Strength for D357-T6.

TABLE 9. D357-T6 EQUIVALENT INITIAL FLAW SIZE DATA.

Foundry	Maximum Stress (ksi)	Cycles to Failure ($x10^3$)	EIFS (inch)
A	30	4069	0.0027
	30*	1474	0.0052
	35	220	0.0103
	45	50	0.0111
	40*	50	0.0159
	40	50	0.0162
	20*	5300+	-
Avg.			0.0102
B	30*	254	0.0150
	40*	45	0.0167
	30	213	0.0168
	20*	982	0.0223
	45	14	0.0228
	25	223	0.0267
Avg.			0.0201

*Glycol-quenched
+No failure

calculated.

The data indicate that the EIFS for Foundry A is less than that for Foundry B. This is consistent with the S/N fatigue data shown in Figure 10; the results for test specimens from Foundry A material are at the higher end of the overall band of data. The EIFS data were then analyzed as described in Section 4.3.3 to determine the value of the maximum inherent material rogue flaw size (99.9% probability and 95% confidence) that should be used to design a cast DADT critical component to a specific life. The data are presented as a Weibull distribution in Figure 15. For D357-T6, the maximum flaw size was determined to be 0.030 inch, which is less than the 0.050 inch flaw that is typically assumed for damage tolerance analysis of wrought materials [7]. A defect of this size may be detected in material up to about 3-inches-thick using X-ray radiography at a 1% sensitivity. Based on this information, Grade B or better D357-T6 castings up to the maximum thickness evaluated under the DADTAC program (1.25 inch) can be considered for use in a damage tolerance design.

The fracture surfaces of the fatigue coupons were examined to determine the size of the crack initiation sites for a comparison to those derived from the EIFS analysis, Table 10. The measured values were obtained by determining the semicircular area within which the flaw would fit with the center of the semicircle on the surface of the specimen. Measured values were not obtained for all twelve fatigue specimens because exact identification of the complete crack site was not possible due to the presence of multiple defects. The derived values are within an order of magnitude of the measured values. Discrepancies between the measured and derived values are most probably due to the inability to accurately account for the effects of the shape (sometimes very complex) and orientation of the crack initiation sites relative to the specimen surface. The difficulty of accurately measuring defects is illustrated in Figures 16a and b. The measured defect size is indicated by the semicircle enclosing

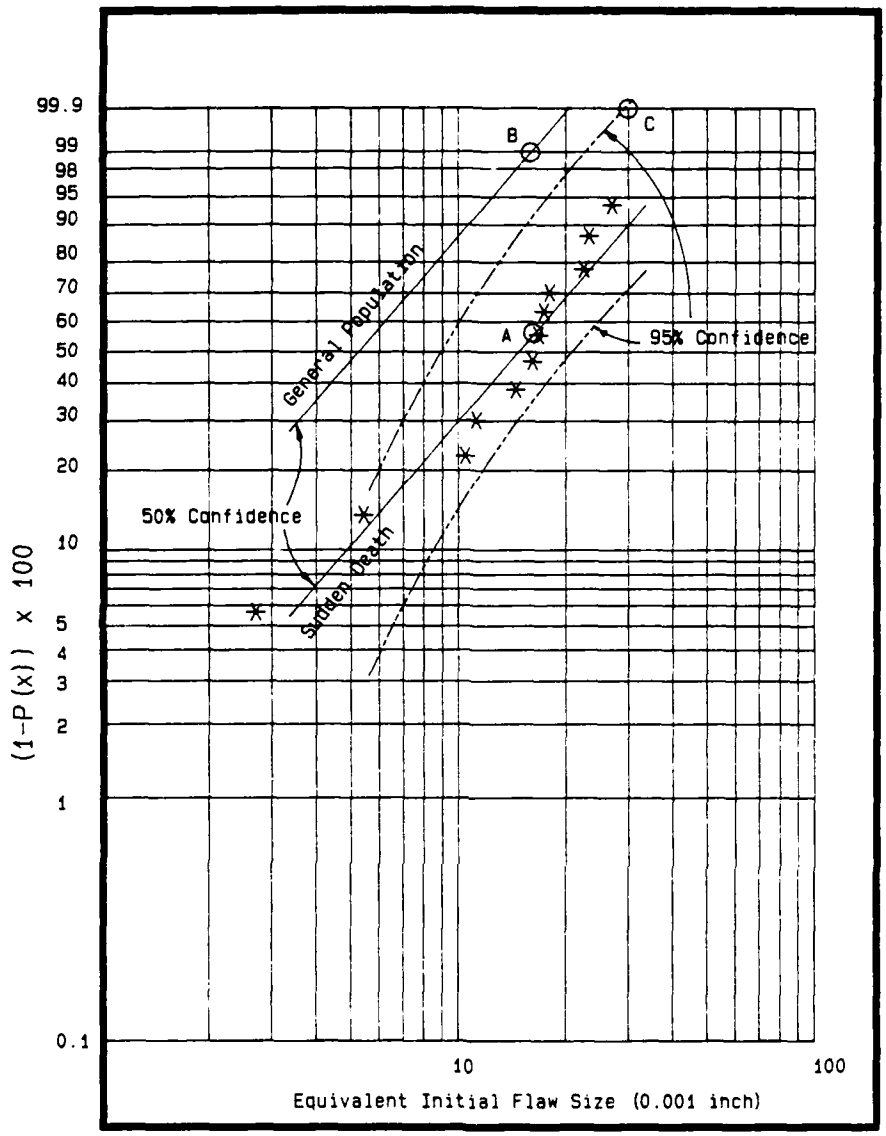

Note: Weibull mean of the sudden death data (A) clusters about the 99% probability level of the general population (B). The maximum (99.9% probability with 95% confidence) expected flaw is indicated by point (C).

Figure 15. Weibull Distribution of D357-T6 EIFS Data.

TABLE 10. COMPARISON OF PREDICTED AND MEASURED EQUIVALENT INITIAL FLAW SIZE FOR D357-T6.

Specimen	EIFS (in)	
	Predicted	Measured
V111	0.0027	0.0175
V115	0.0052	0.0375
V116	0.0159	0.0343
V209	0.0229	0.0096
V210	0.0267	0.0162
V211	0.0150	0.0062
V213	0.0223	0.0137

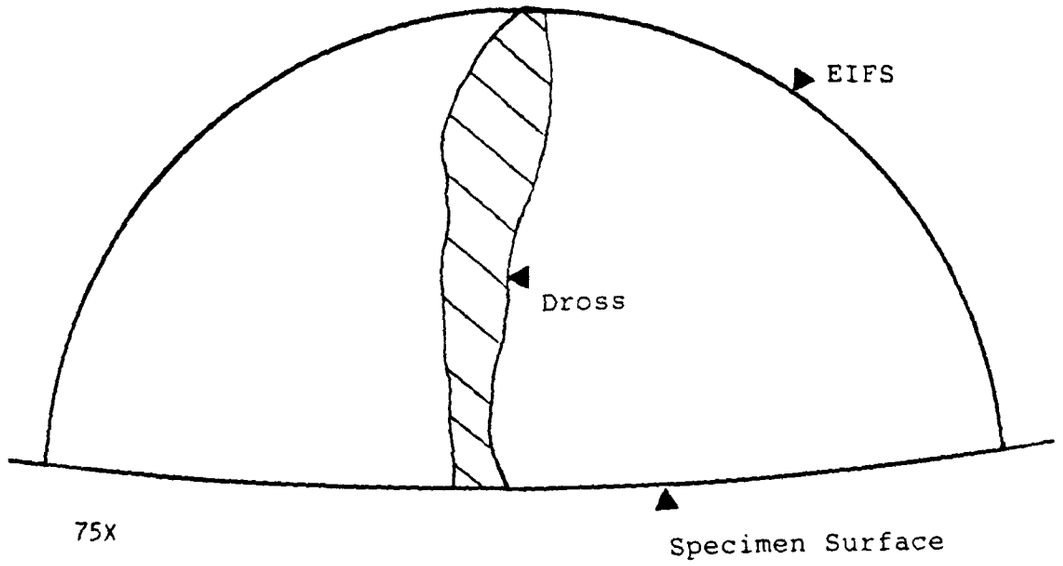

a. Dross.

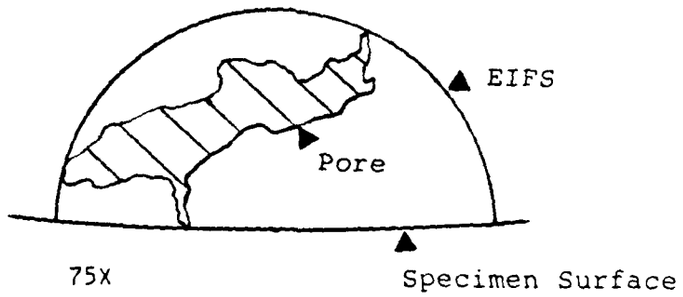

b. Pore.

Figure 16. Measurement of Defect Size in D357-T6.

each defect with the center of the semicircle placed on the edge of the specimen. (A semicircle was used because DADT analyses assumes the presence of a semicircular flaw in the material.) It can be clearly seen that the semicircle encloses much more material than the defect, and that the size of the semicircle is highly dependent upon the aspect ratio of the defect. In contrast, the EIFS analysis determines the semicircular area which has the same effect on fatigue properties as a highly aspected defect. Highly aspected defects can cause the measured defect size to be either greater than or less than the predicted defect size (the EIFS). From this comparison, it was concluded that the approach being used to predict the EIFS from smooth fatigue data is viable.

5.2 B201-T7 RESULTS

5.2.1 Composition

Twenty plates cast (both 1.25-inch-thick and 0.75-inch-thick) from eight different melts by three foundries were used for the B201 verification evaluations. The composition of each of these melts and the ranges for each element are listed in Table 11. All of the compositions were within the specified range (AMS 4242). Reported compositions of the plates were confirmed by ICP tests at Northrop.

5.2.2 Microstructure

The microstructure of the B201-T7 plates was characterized using optical, TEM, STEM, and SEM methods, and the grain size and percent porosity of each plate were determined.

The grain size at random locations in plates from all three foundries ranged from 0.0024 inch to 0.0039 inch. A typical micrograph of the B201-T7 microstructure is shown in Figure 17.

TABLE 11. B201 VERIFICATION MATERIAL MELT COMPOSITIONS.

COMPOSITION (wt %)							
Cu	Ag	Mg	Mn	Ti	Fe	Si	Al
4.59	0.56	0.27	0.28	0.19	0.02	0.04	Bal.
4.55	0.55	0.30	0.28	0.18	0.01	0.02	Bal.
4.54	0.40	0.27	0.22	0.17	0.01	0.05	Bal.
4.75	0.44	0.24	0.33	0.16	0.02	0.05	Bal.
4.69	0.64	0.28	0.28	0.28	0.04	0.04	Bal.
4.93	0.69	0.28	0.28	0.28	0.04	0.04	Bal.
4.59	0.65	0.26	0.27	0.24	0.04	0.02	Bal.
4.63	0.57	0.25	0.31	0.18	0.02	0.01	Bal.
AMS 4242 Specification							
4.5-5.0	0.40-0.80	0.20-0.30	0.20-0.50	0.15-0.35	≤0.05	≤0.05	Bal.

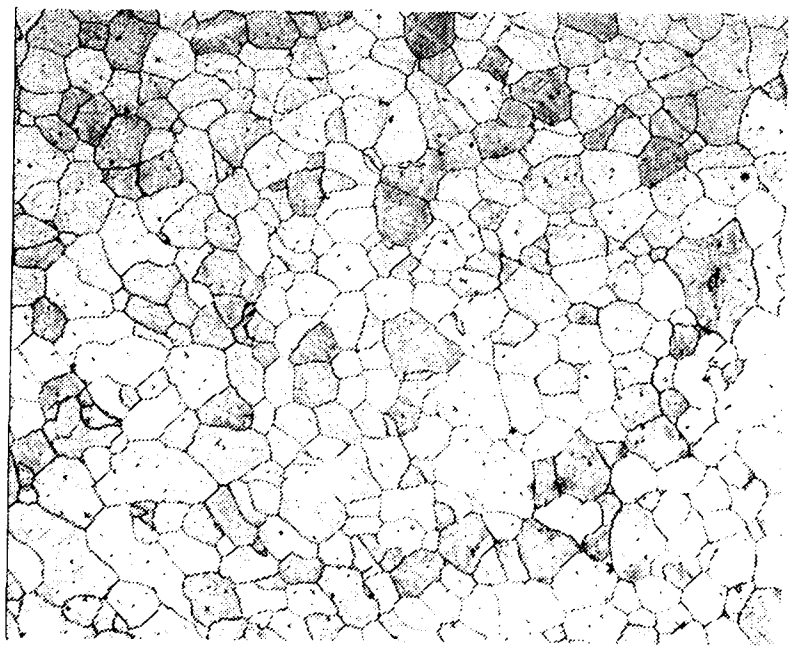

50X Kellers etch

Figure 17. Typical B201-T7 Microstructure.

The microstructure was examined further by SEM, STEM, and TEM. SAD diffraction patterns and EDXA of various phases were taken, leading to the identification of five different phases. The most prominent of these five was the strengthening phase $CuAl_2$, (theta), Figure 18, found as small platelets on the (100) plane of the aluminum matrix. A grain boundary phase and associated precipitate-free zone were also observed in Figure 18. EDX analysis of the grain boundary area identified the presence of Al and Cu, suggesting the phase was equilibrium $CuAl_2$. $CuAl_2$ was also seen as a large blocky constituent phase, Number 2 in Figure 19. Other large constituents were also observed in Figure 19. The constituent labeled Number 1 contained Cu and Fe. The constituents indicated by Numbers 3 and 4 were rich in Ti, and those indicated by Numbers 5 and 6 contained Cu, Fe, and Mn.

Two grain boundary phases were also observed in addition to the equilibrium $CuAl_2$ phase. One was the Al, Cu, Fe, and Mn rich phase mentioned previously, Number 1 in Figure 20; the other was rich in Al, Cu, and Mn, Number 2. A large blocky Al, Cu, and Mn phase was also observed in the matrix, Figure 21. Figure 22 shows another Al-Ti phase, which was either Al_3Ti, $Al_{24}Ti_6$, or $Al_{23}Ti_9$.

The $CuAl_2$ phase identified above has been reported [15] for alloys containing Ag to be omega, an altered form of theta, the main strengthening precipitate in Al-Cu alloys. The addition of Ag to Al-Cu alloys promotes the formation of the omega strengthening precipitate during aging above about 210F and causes a marked increase in age hardening. Silver was also shown by regression analyses [1] to increase the strength of B201-T7. Omega essentially replaces theta and is thought to be a monoclinic or hexagonal form of the theta phase, which itself is body-centered tetragonal. Omega forms on the (111) plane of the matrix as a uniform dispersion of large, very thin, hexagonally shaped plates, and is thought to be coherent with the matrix along the (111) plane and at the ends of the precipitate. Omega

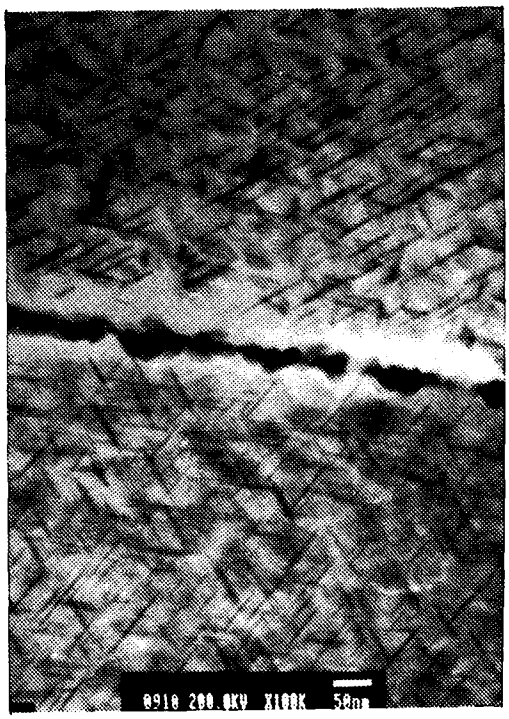

Figure 18. TEM Micrograph of B201-T7 Showing the Theta Phase.

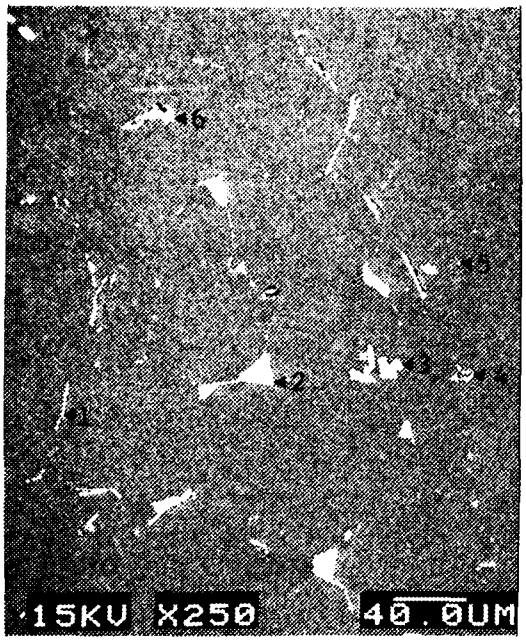

Figure 19. Backscatter SEM Image of B201-T7.

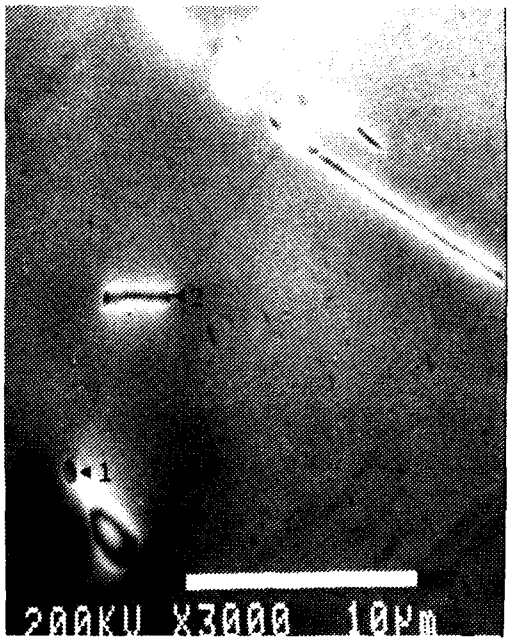

Figure 20. STEM Micrograph of B201-T7 Showing a Phase Rich in Al, Cu, Fe, and Mn.

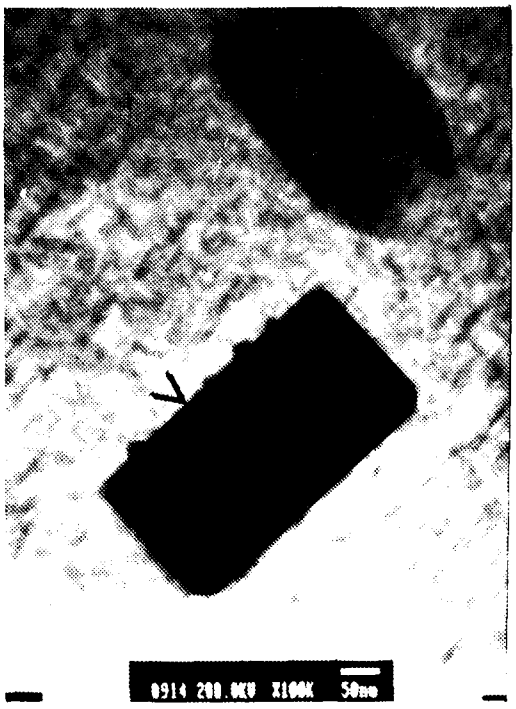

Figure 21. TEM Micrograph of B201-T7 Showing a Phase Rich in Al, Cu, and Mn.

Figure 22. TEM Micrograph of B201-T7 Showing a Phase Rich in Al and Ti.

may be more stable than theta, as evidenced by creep testing [15]. In addition, the precipitation mechanism associated with the omega phase seems to be different from that of the theta phase.

Scanning diffractometry of B201 was also conducted to identify phases. Analysis of the diffraction pattern led to the identification of only two phases, Al_2O_3 and delta (Al_4Cu_9). Phases containing other alloying elements were not detected due to the relatively small amount (<1 wt percent) of all alloying elements in B201 except for Cu.

5.2.3 Tensile Properties

The average and minimum (indicated by the ranges) tensile properties of the 1.25-inch-thick B201-T7 plates from all three foundries are shown in Table 12. Test results were also obtained for the 0.75-inch-thick plates to provide a direct comparison with those obtained in the screening portion of Task 2. Average tensile properties of 66.5 ksi ultimate strength, 59.1 ksi yield strength, and 8.3 percent elongation to failure were obtained for the 0.75-inch-thick verification plates with minimum values of 64/55/6.5. These properties are similar to those obtained for the screening material (65/57/7).

All the individual tensile properties for the 1.25-inch-thick verification plates from all three foundries exceeded the specified minimum of 60 ksi ultimate strength, 50 ksi yield strength, and 3 percent elongation. Material from Foundry B had the highest strength; material from Foundries A and C had similar properties. Stress corrosion tests were conducted (Section 5.3.6) and confirmed that the alloys were in the T7 condition.

TABLE 12. TENSILE PROPERTIES OF 1.25-INCH-THICK B201-T7 PLATES.

Foundry	UTS (ksi)		YS (ksi)		El (%)	
	Avg.	Range	Avg.	Range	Avg.	Range
A	66	65-67	57	54-58	8.7	8.3-11.0
B	70	68-73	63	60-66	8.2	7.5-8.8
C	67	64-70	60	58-62	8.3	6.5-9.5
Average	68		60		8.4	
Target Min.	60		50		3.0	

5.2.4 Fatigue Properties

5.2.4.1 Smooth Stress-Life

The stress-life (k_t=1.0) data for B201-T7 from the three foundries are shown in Figure 23, along with a comparison to data for A201-T7 material obtained under a previous Northrop/Navy contract [16], and 7075-T73 [11], an alloy commonly used in fatigue-critical aircraft applications. The fatigue lives for B201-T7 from the three foundries are similar and are essentially the same as the previous results [16]. However, the fatigue life for a given stress was shorter than that of 7075-T73.

5.2.4.2 Smooth Strain-Life

The strain-life data, plotted as log strain amplitude vs. log of the number of cycles to failure (N_f), are shown in Figure 24. The specimens were tested using an R ratio of -1.0, with strain amplitudes ranging from 0.008 to 0.002. These strain amplitudes resulted in fatigue lives ranging from approximately 500 to 200,000 cycles. These data were generated for use in the durability analysis to be conducted later in the program (described in Section 4.3.2).

5.2.4.3 Fatigue Crack Growth Rate

The range of fatigue crack growth rate (constant amplitude) data for B201-T7 from the three foundries is shown in Figure 25. Also included are data for A201-T7 tested under a Northrop/Navy contract [16], and 7075-T7351 plate [13], an alloy used in fatigue critical aircraft applications. The DADTAC program data are similar to the Northrop/Navy contract A201-T7 data. However, B201-T7 had a slightly slower fatigue crack growth rate than 7075-T7351. Because the FCGR for castings and 7075-T7351 is similar, the difference in total fatigue life (Figure 23) can be attributed to the reduced crack initiation resistance of the cast

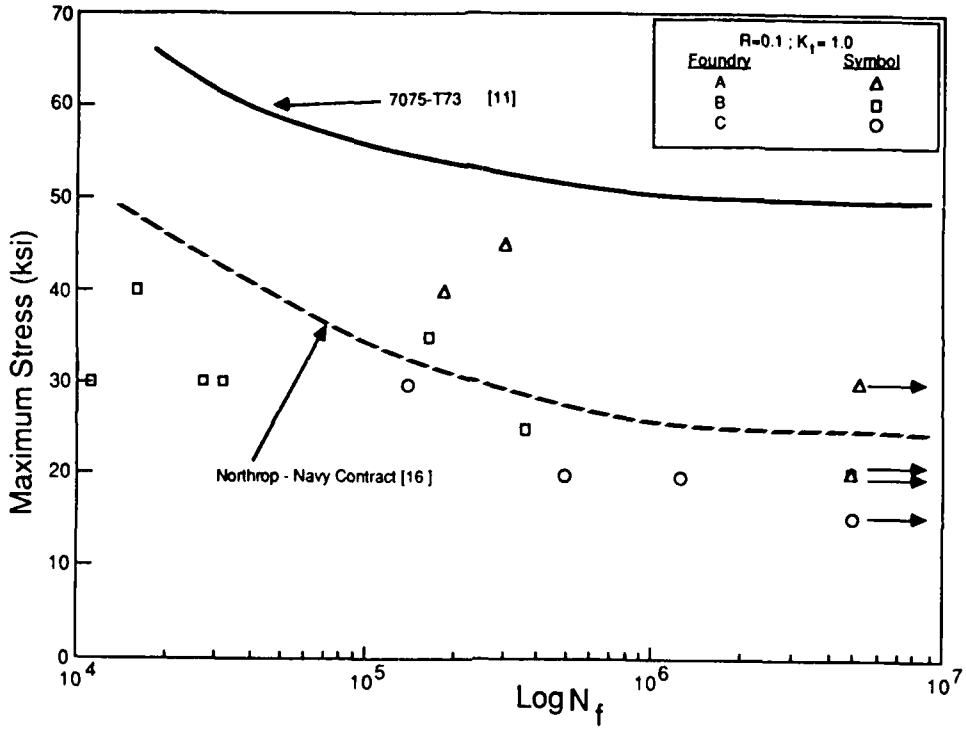

Figure 23. B201-T7 Stress-Life Fatigue Data.

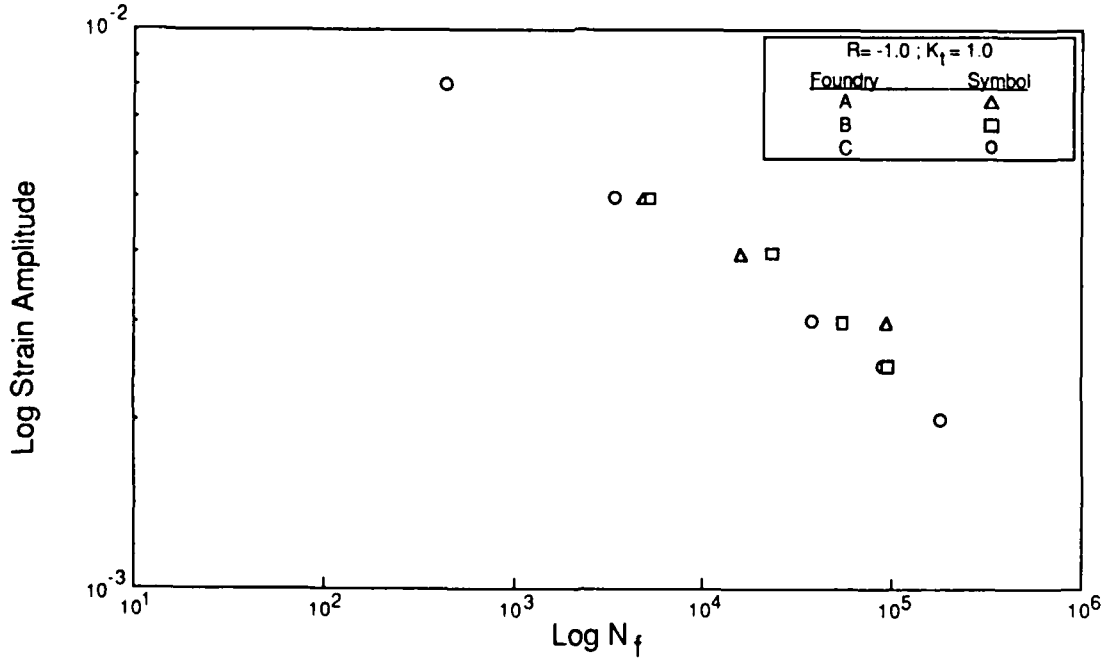

Figure 24. B201-T7 Strain-Life Fatigue Data.

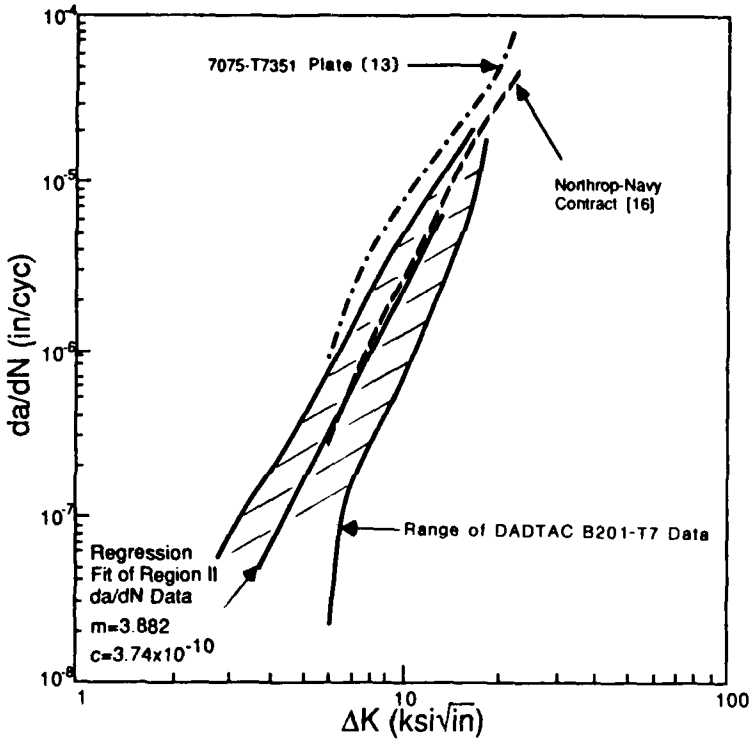

Figure 25. B201-T7 Fatigue Crack Growth Rate Data (R=0.1; lab air).

material, which is presumably due to the presence of inherent defects such as dross and/or porosity.

Each fatigue life specimen was fractographically examined to determine the crack initiation site(s). Out of eight specimens examined, fatigue cracks in seven of them initiated at defects. It was not possible to detect a defect associated with the crack initiation in the remaining specimen. The defects were either gas porosity, residual shrink porosity, or foreign material. A typical foreign material defect is shown in Figure 26.

5.2.5 Fracture Toughness

Average compact tension and short bar fracture toughness values, as well as NTS/YS ratios, of B201-T7 are shown in Table 13. The short bar test specimens were excised from the broken compact tension specimens to provide a direct comparison of the two test methods. An average K_Q value of 39.4 ksi$\sqrt{in}$ was obtained from compact tension testing, which is similar to the average K_{IV} value of 40.4 ksi $\sqrt{in}$ obtained from the short bar test. The average K_Q values for Foundries A, B, and C were 43, 29, and 47 ksi $\sqrt{in}$, respectively.

Invalid K_Q results were obtained for all the compact tension tests due to excessive crack front curvature, similar to the WQ D357-T6 specimens (Section 5.1.5).

Individual specimen data and the relationship between fracture toughness and yield strength is shown in Figure 27. The fracture toughness decreased with increasing yield strength and ranged from 27 to 46 ksi$\sqrt{in}$. The corresponding short bar results ranged from 27 to 58 ksi $\sqrt{in}$.

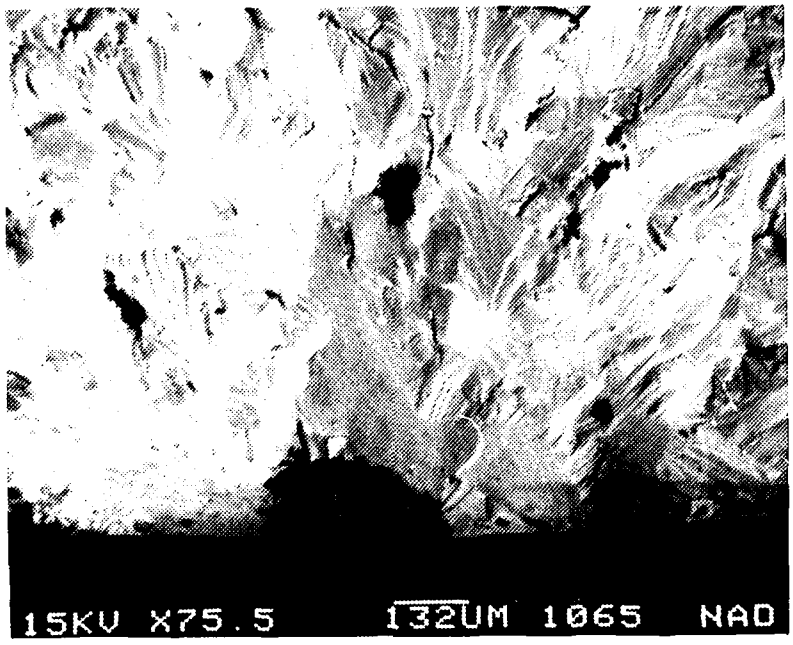

Figure 26. Foreign Material on a B201-T7 Fatigue Specimen Fracture Surface.

TABLE 13. B201-T7 FRACTURE TOUGHNESS DATA.

FRACTURE TOUGHNESS (ksi $\sqrt{in}$) K_Q	K_{IV}*	NTS (ksi)	YS (ksi)	NTS/YS
39.7	40.4	87.3	60.3	1.45

* Short bar test

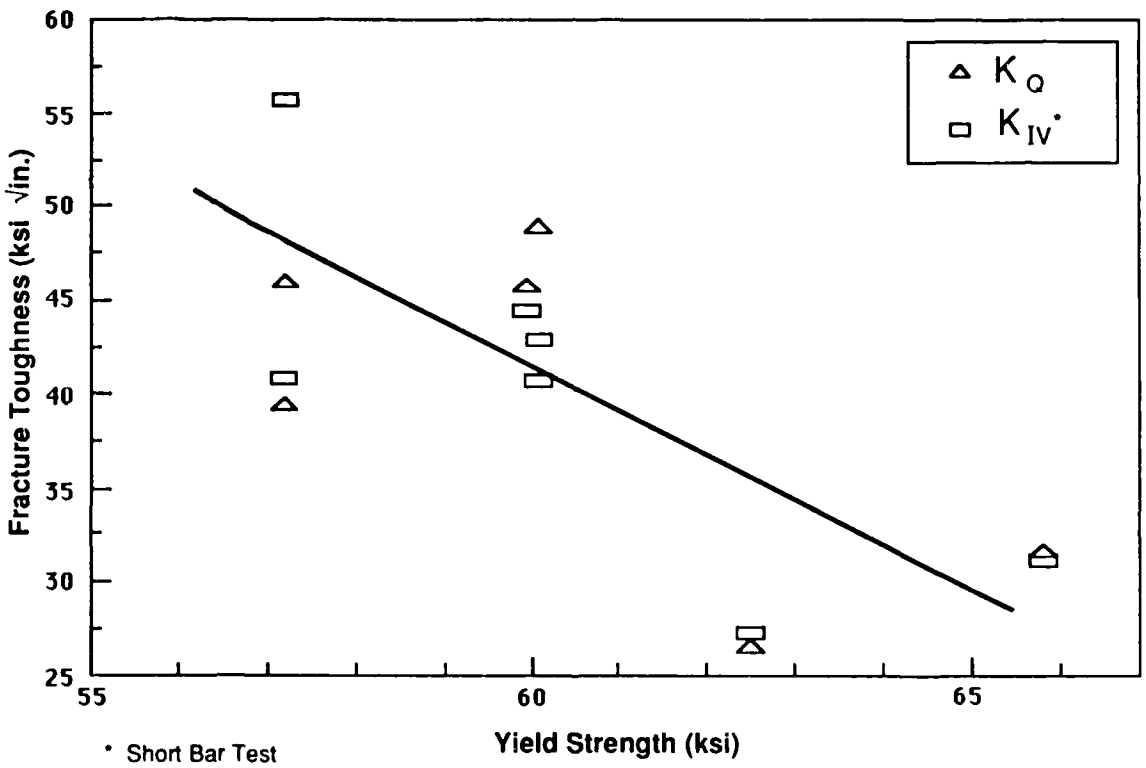

Figure 27. Relationship Between Fracture Toughness and Yield Strength of B201-T7.

5.2.6 Stress Corrosion

Stress corrosion tests were conducted on B201 from all three foundries. Direct tension, alternate immersion tests were conducted; specimens were exposed to a 3.5% NaCl solution for 30 days at 75% of the material yield strength. No failures were experienced after the 30 day exposure, indicating that each plate had been heat treated to the T7 (overaged) condition.

5.2.7 Equivalent Initial Flaw Size Analysis

The method for determining the equivalent initial flaw size was described in Section 4.3.1. The calculated values for individual specimens excised from material from each of the three foundries are shown in Table 14, along with the fatigue life and maximum applied stress. Testing of specimens that did not fail after $5x10^6$ cycles was terminated and an EIFS was not calculated.

The data indicate that the EIFS for material from Foundry A is less than that for Foundries B and C material. This is consistent with the stress-life fatigue data shown in Figure 23; the results for Foundry A material are at the higher end of the overall data band. Data for Foundries B and C are nearly equivalent.

The EIFS data were then analyzed as described in Section 4.3.3 to determine the value of the maximum inherent rogue flaw size (99.9% probability and 95% confidence) that should be used to design a cast DADT critical component to a specific life. The data are presented as a Weibull distribution in Figure 28. For B201-T7, the maximum flaw size was determined to be 0.042-inch, which is less than the 0.050 inch flaw that is typically assumed for damage tolerance analysis [7]. A flaw of this size can be detected in material up to about 4-inches-thick by X-ray radiography using 1% sensitivity. Based on this information, Grade B or better B201-T7 castings up to the maximum thickness

TABLE 14. B201-T7 EQUIVALENT INITIAL FLAW SIZE DATA.

Foundry		Maximum Stress (ksi)	Cycles to Failure ($x10^3$)	EIFS (inch)
A		40	187	0.0037
		45	309	0.0014
		30	5,000*	-
		20	5,000*	-
	Avg.			0.0025
B		25	39	0.0111
		30	28	0.0404
		35	188	0.0067
		20	5,000*	-
	Avg.			0.0194
C		40	16	0.0289
		20	118	0.0086
		20	573	0.0160
		30	168	0.0118
		15	5,000*	-
	Avg.			0.0163

*No Failure

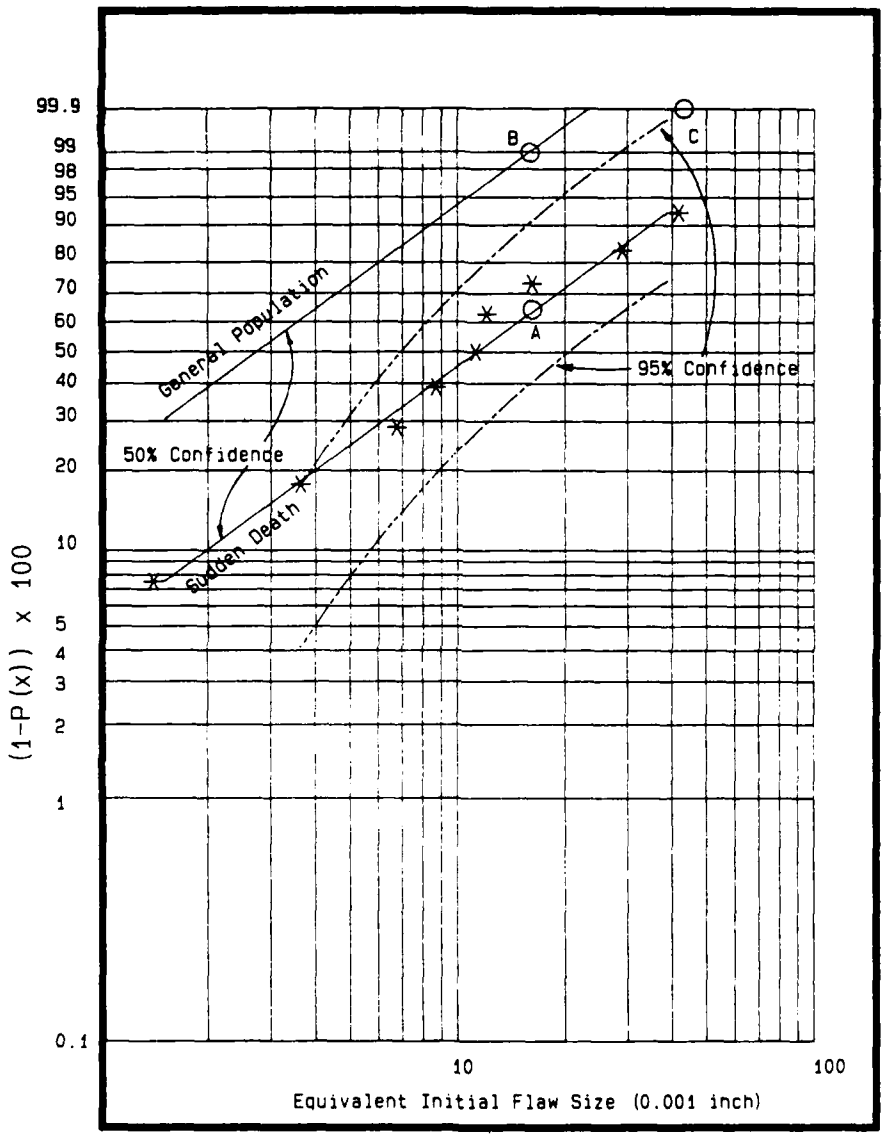

Note: Weibull mean of the sudden death data (A) clusters about the 99% probability level of the general population (B). The maximum (99.9% probability with 95% confidence) expected flaw is indicated by point (C).

Figure 28. Weibull Distribution of B201-T7 EIFS Data.

evaluated under the DADTAC program (1.25 inch) can be considered for use in a damage tolerance design.

The fracture surfaces of the fatigue coupons were examined to determine the size of the crack initiation sites. A comparison of these measured values and those derived from the EIFS analysis is shown in Table 15. The measured values were obtained by determining the semicircular area within which the flaw would fit, with the center of the semicircle on the surface of the specimen. The derived values are within an order of magnitude of the measured values. Discrepancies between the measured and derived values are probably due to the inability to accurately account for the effects of the shape and orientation of the crack initiation sites as was discussed previously in Section 5.1.6.

TABLE 15. COMPARISON OF PREDICTED AND MEASURED EQUIVALENT INITIAL FLAW SIZE FOR B201-T7

Specimen	EIFS (in)	
	Predicted	Measured
V156	0.0037	0.0025
V256	0.0111	0.0037
V355	0.0118	0.0366
V356	0.0086	0.0316
V357	0.0160	0.0075

SECTION 6
CONCLUSIONS

1. Tensile properties of the verification material produced using the specifications derived from the screening portion of Task 2, which were similar to AMS specifications 4241 and 4242 except for the addition of a Si modifier for D357-T6, were similar to those of the screening plates. Thus, the specifications can be met by the foundries, and are valid for material of a thickness up to that evaluated in this program (1.25-inches-thick).

2. The fatigue crack growth rates of D357-T6 and B201-T7 castings are similar, but are slightly slower than those of 7075-T7351.

3. Based on an evaluation of the smooth fatigue (k_t=1.0) specimen fracture surfaces, the overall fatigue life, and the FCGR, crack initiation occurs sooner in castings than in 7075-T7351 due to the presence of inherent defects.

4. The equivalent initial flaw size for D357-T6 (0.030-inch) and B201-T7 (0.042-inch) is less than the value assumed for wrought alloys (0.050-inch). For castings up to 1.25-inch-thick, these alloys can be considered for damage tolerance applications based on the existing damage tolerance specifications (MIL-A-83444 and MIL-A-87221).

5. The average fracture toughness (K_Q) of D357-T6 was adequate (24 ksi$\sqrt{in}$). Though the average value for B201-T7 was excellent (40 ksi$\sqrt{in}$), there was significant foundry-to-foundry variability, ranging from 20 to 47 ksi$\sqrt{in}$.

6. Excellent agreement between results of the compact tension and short bar fracture toughness tests was attained.

SECTION 7
REFERENCES

1. M.W. Ozelton and G.R. Turk, "Durability and Damage Tolerance of Aluminum Castings," First Interim Report, Contract No. F33615-85-C-5015, September, 1987.

2. Aerospace Materials Specification, AMS 4241, 1986, Society of Automotive Engineers, Warrendale, PA 15096.

3. Aerospace Material Specification, AMS 4242, 1986, Society of Automotive Engineers, Warrendale, PA 15096.

4. "Determination of Dendrite Arm Spacing in Aluminum Castings," Northrop Process Specification IT-72.

5. P.G. Porter, "A Unified Approach to Crack Initiation and Growth Analysis," Northrop Report No. NOR 87-102, October, 1987.

6. "Northrop Fatigue/Damage Tolerance Manual," Vol. I, Section III.

7. "Airplane Damage Tolerance Design Requirements," MIL-A-83444, July, 1974.

8. Lipson, C. and Sheth, N.J., "Statistical Design and analysis of Engineering Experiments," Section 5.5, McGraw-Hill, 1973.

9. "Fatigue-Endurance Data," Vol 2., Aeronautical Series of Engineering Sciences Data, Item No. 68016, The Royal Aeronautical Society, London, England, 1968.

10. Polmear, I.J., "Light Alloys - Metallurgy of the Light Metals," ASM International, Metals Park, OH, 1982, p. 119.

11. Northrop IR&D Program 85-R-1098.

12. Unpublished Data, Northrop Aircraft Division.

13. Northrop IR&D Program 84-R-1098.

14. Unpublished Data from the Premium Casting Task Force, AFS Committe 2D.

15. Polmear, I.J., "Development of an Experimental Wrought Aluminum Alloy for use at Elevated Temperatures," V. 1, pp. 664-665, published in Aluminum Alloys, Their Physical and Mechanical Properties, proceedings of an International Conference at University of VA, June, 1986.

16. Scarich, G.V. and Wu, K.C. "Hot Isostatic Pressing of Aluminum Castings," Final Report, Contract N00019-80-C-0276, February, 1986.